Quantum Invariants and Geometric Structure of 3-manifolds

量子不変量と3次元多様体の幾何構造

March 2006

Koji Ohnuki

大貫　浩二

Research on Topology,
Major in Mathematical science,
Graduate School of Science and Engineering,
Waseda University,
Tokyo, Japan

Acknowledgements

I would like to expresses great gratitude to Professor Jun Murakami who gave me very warm and constant encouragements and guided the study of the volume conjecture.

I would also like to express my thanks to Professor Yoshiyuki Yokota for many valuable advice on the work in Chapter 2.

Finally, I am grateful to my parents, my brothers and my friends.

Koji OHNUKI
Major in Mathematical Science
Graduate School of Science and Engineering
Waseda University
3-4-1, Okubo, Shinjuku-ku
Tokyo, 169-8555
JAPAN

Introduction

A knot is mathematically defined as an embedded circle in the three-sphere. This object is very familiar with us and we can see many knots in our daily life. It is natural to ask how many knots there are. In Knot theory we want to classify knots as mathematical objects.

In Algebraic topology developed by Poincaré we can distinguish one topological space from the other by using topological invariants as the homology group or the fundamental group. Therefore it seems to be useful to distinguish one knot from the other by using some invariants. Many invariants for knots are discovered by many mathematicians. Classically the Alexander polynomial was defined by using the homology theory. This is an isotopy invariant such that a knot is mapped to a polynomial ring.

The discovery of the Jones polynomial in 1984 was a turning point in the study of knot invariants. The Jones polynomial is discovered from the study of operator algebras, not from topology. The discovery of the Jones polynomial led many discoveries of new knot invariants, and interaction between knot theory and other fields as representation theory and mathematical physics. In fact new knot invariants are defined by the solution of the Yang-Baxter equation in statiscal mechanics and the representation of quantum groups, and they are all called by quantum invariants of knots.

We have many quantum invariants. Actually for a Lie algebra we can construct a quantum invariant by finding the solution of the Yang-Baxter equation. Moreover the Alexander polynomial which is defined by the homology theory is also defined as a quantum invariant.

In this thesis, we discuss the relation between quantum invariants and geometric structures on 3-manifolds. In particularly, we will consider the volume conjecture that the colored Jones polynomial relates the volume of the complement of knot in the three-sphere.

The colored Jones polynomial is one of link invariants which includes the Jones polynomial. It is obtained from the quantum group $\mathcal{U}_q(sl_2)$ and it's irreducible representation.

Let L be an oriented link and N be a positive integer. We can calculate the colored Jones polynomial of L denoted by $J_N(L; q)$ as follows. First we present L into a (1,1)-tangle T by cutting a component. Next we label each edge of T an element in $\{0, 1, \ldots, N-1\}$. Here two edges containing end points of T are labelled 0. We assign each crossing and each edge containing a local maximal point or minimal point to some values. After multiplying these values obtained from the tangle we take a sum over all labels so that we have the colored Jones polynomial $J_N(L;q)$.

We have no explicit geometric interpretation of the quantum invariant but the volume conjecture implies some relation between the colored Jones polynomial and the geometric invariant of knot exterior.

R. Kashaev defined a series of complex valued invariants of a link for the integer N from the study of the quantum dilogarithm, and he conjectured that for any hyperbolic link the asymptotic behavior of his link invariants determines the volume of the complement of the link in the three-sphere S^3. By using the saddle point method he checked his conjecture for 4_1, 5_2, and 6_1, but unfortunately his argument is not justified mathematically.

In [25], it was proved that Kashaev's link invariant is equal to the special value of the colored Jones polynomial which is also equal to the specializations of the Akutsu-Deguchi-Ohtsuki invariant ([1]), and Kashaev's conjecture was extended to the volume conjecture that for any knot the asymptotic behavior of the colored Jones polynomial determines the simplicial volume of the complement of a knot in S^3. It is known that this conjecture is true for the figure eight knot. Moreover R. Kashaev and O. Tirkkonen showed that the volume conjecture holds for torus knots which are known as non-hyperbolic knots. Also it was proved in [6] that the volume conjecture for the Borromean rings is true. In [26], it was numerically observed that the colored Jones polynomials are related to the volumes and the Chern-Simons invariants of the complements of some knots and the Whitehead link. In [22], it was suggested that the Witten-Reshetikhin-Turaev invariants for closed manifolds obtained from the figure-eight knot by Dehn surgery are related to the volumes and the Chern-Simons invariants.

On the other hand, in [35] D. Thurston introduced the ideal triangulation of the complement of a hyperbolic knot related to it's Kashaev invariant or it's colored Jones polynomial. In [39] Y. Yokota showed that the hyperbolicity equations coincide with the equations obtained in the process of analyzing the asymptotic behavior of Kashaev invariants by using the saddle point method.

Recently we considered some generalization of the volume conjecture. We expect that the asymptotic behavior of the colored Jones polynomial $J_N(L;q)$ evaluated at $q = \exp(2\pi\alpha\sqrt{-1}/N)$ with a fixed complex parameter α determines the some geometric invariant of 3-manifolds obtained from the knot. In fact for the figure-eight knot it was proved in [23] that if α is real that determines the volume of the cone-manifold with singurality along the figure-eight knot. Moreover it was proved in [27] that if α is complex number the colored Jones polynomial determines the Neumann-Zagier function.

This thesis is separated into 3 chapters.

In Chapter 1, we review how to construct quantum invariants and state the volume conjecture.

In Chapter 2, we discuss the relation between a colored Jones polynomial of an alternative 2-bridge link and its hyperbolic structures.

Due to W. Thurston [36], hyperbolic structures of a three-manifold which is decomposed into ideal tetrahedra can be described as algebraic equations. Here an ideal tetrahedron is the tetrahedron whose vertices are on the sphere at infinity. We can prametrize the ideal tetrahedron as a complex number z by putting its 4 vertices at $(0,0)$, $(1,0)$, $(z,0)$ and ∞ in the upper half space $\mathbb{C}\times\mathbb{R}$. Dihedral angles of the ideal tetrahedron are parametrized by z are z, $1-\frac{1}{z}$ and $\frac{1}{1-z}$.

We can describe hyperbolic structures of the complement of a knot in the three-sphere as algebraic equations as follows.

First, we construct the ideal triangulation for the knot complement and associate each tetrahedra with complex parematers. Next, we give hyperbolic structures on the knot complement. To do this we neatly glue a tetrahedron each other. This means that the sum of dihedral angles around an edge is 2π. We can describe this condition by algebraic equations because the product of parameters associated to ideal tetrahedra is equal to 1. Next, we consider the completeness. This condition is that the neighbourhood of knot that is a torus is Euclidian and we also describe this condition by algebraic equations for parameters associated to ideal tetrahedra. These algebraic equations are called hyperbolicity equations. By solving hyperbolicity equations we give the complete hyperbolic structure on the knot complement. And we compute the hyperbolic volume of the knot complement by taking the sum of the volume of ideal tetrahedra which give the complete hyperbolic structure.

Now, following D. Thurston [35] and Y. Yokota [39], we give ideal triangulation for the complement of a 2-bridge knot L in the three-sphere.

First, we put an octahedron at each crossing of L. Each octahedron is decomposed into 5 tetrahedra and two vertices of an octahedron are tangent to L. Next we deform each octahedron by identifying two pairs of edges and glue two faces in opposition to each other along a knot. Then we have the ideal triangulation of the three-sphere without L and two points $\{\pm\infty\}$. If we remove the neighbourhood of a pairs of two faces which include $\{\pm\infty\}$ as a vertex then we have the ideal triangulation for the complement of L. This ideal triangulation is corresponding to the R-matrix used in computing the colored Jones polynomial. Also the ideal triangulation corresponding to Kashaev's R-matrix is constructed in [39].

Next we describe hyperbolicity equations for this ideal triangulation. We note that this hyperbolicity equations are coincide with the hyperbolicity equations for the canonical decomposition of the complement of L constructed in [34]. But we can see that the ideal triangulation corresponding to the colored Jones polynomial is different in configuration from the canonical decomposition.

Now, we calculate the colored Jones polynomial of a 2-bridge link as above. In [10], we express the sum of q-integer the multi-integral and approximate this sum for the large N by using the saddle point method. This method is not justified completely, but we give the geometric interpretation to the function obtained when we apply the saddle point method to the multi-integral formula for the colored Jones polynomial or Kashaev's invariant. When we approximate the colored Jones polynomial in Kashaev's way we consider algebraic equations obtained from the derivatives of this function. In Chapter 2, we will see that these algebraic equations obtained from the colored Jones polynomial of a 2-bridge link are corresponding to the hyperbolicity equations for the complement of the link in the three-sphere. On the other hand, we can describe the volume of the link complement as the sum of volumes of ideal tetrahedra and compare it with the critical value of the function obtained from the colored Jones polynomial. Summarizing above, we will prove the following theorem in Chapter 2.

Theorem 2.1. *For the alternating 2-bridge link, $V(z_2,\dots,z_{c_n-2},w)$ denotes the function obtained from the colored Jones polynomial by Kashaev's way. Then the system of the equations* $\left\{\exp\left(z_j\dfrac{\partial V}{\partial z_j}(z_2,\dots,z_{c_n-2},\infty)\right)=1\right\}_{j=2,\dots,c_n-2}$ *coincides with the hyperbolicity equations.*
If $(\zeta_2,\dots,\zeta_{c_n-2})$ is the solution of the equations such that $\mathrm{Im}(\zeta_j)>0$, then

$$\mathrm{Vol}(S^3-L)=-\mathrm{Im}(V(\zeta_2,\dots\zeta_{c_n-2},\infty))\,.$$

Here, we will find an extra-parameter w in this theorem. In the case of Kashev's invariant [39], there is no extra-parameter and hyperbolicity equations coincide with algebraic equations. This extra-parameter is due to the tangle presentation in the computation of the colored Jones polynomial. If we take the good tangle presentation, we remove this extra-parameter by using formulas for the sum of q-integer. Also we can calculate colored Jones polynomials by using the skein theory [14, 18]. By using the skein theory we sometimes have a simple formula for the colored Jones polynomial. But we have no geometric interpretation of this formula uniformally. Finally, we will give this geometric interpretation in the case of twist knots.

In Chapter 3, we consider a generalization of the volume conjecture. We consider the case of the Borromean rings B. Let $\Lambda(z)$ be the Lobachevsky function and two functions $V_1(r)$ and $V_2(r)$ as follows.

$$\begin{aligned} V_1(r) &= 2\left(3(\Lambda(\pi r+\theta)-\Lambda(\pi-\theta))-4\Lambda(\theta+\pi/2)-2\Lambda(\theta)\right),\\ V_2(r) &= 2\left(-3(\Lambda(\phi+\pi r)+\Lambda(\phi-\pi r))+4\Lambda(\phi+\pi/2)+2\Lambda(\phi)\right), \end{aligned}$$

where $\theta=\theta(r)$ and $\phi=\phi(r)$, $0<\theta,\phi<\frac{\pi}{2}$ are principal parameters defined by conditions

$$\begin{aligned} &T=\tan\theta,\ T^4-(3\tan^2(\pi r)+1)T^2-\tan^6(\pi r)=0,\\ &T'=\tan^2\phi,\\ &T'^3-3\tan^2(\pi r)T'^2+(\tan^6(\pi r)+6\tan^4(\pi r)+3\tan^2(\pi r)+1)T'-\tan^6(\pi r)=0. \end{aligned}$$

Let r_1 and r_2 be the solution of the equation $V_1(r)=V_2(r)$ and $0<r_1<r_2<1$. In Chapter 3, we will prove the following theorem.

Theorem 3.1. *Let r be the irrational number satisfying $r_2 < r < 1 + r_1$. Then*

$$2\pi \lim_{N\to\infty} \frac{\log\left|J_N(B;\exp(2\pi r\sqrt{-1}/N))\right|}{N} = \frac{1}{r}V_1(r).$$

Here $V_1(r)$ coincides with the hyperbolic volume of the cone manifold whose underlying space is the three-sphere and whose singular set consists of three components of the Borromean rings with cone angles $2\pi|1-r|$, $2\pi|1-r|$ and $2\pi|1-r|$ [19].

Finally, we will see some numerical examples of $\dfrac{\log J_N(L;\exp(2\pi r\sqrt{-1}/N))}{N}$ for the Borromean rings and the Whitehead link. These examples shows that the colored Jones polynomial evaluated at $\exp(2\pi r\sqrt{-1}/N))$ for the real number r relates the hyperbolic volume of the cone manifolds which admit the hyperbolic structure.

Contents

Chapter 1

Quantum invariants of knots

In this chapter we review quantum invariants and some examples. In Section 4, We state the volume conjecture.

1.1 Topology of knots and links

A knot is the image of a smooth embedding $S^1 \to \mathbb{R}^3$ and a link is the image of a smooth embedding of the disjoint sum of circles into $\mathbb{R}^3$. Two knots or links K and K' are called isotopic if there exists a smooth (or piecewise smooth) map $h : \mathbb{R}^3 \times [0,1] \to \mathbb{R}^3 \times [0,1]$ such that $h(x,0) = x$ and $h(K,1) = K'$. In other words, two knots or links K and K' are isotopic if K is obtained from K' by the continuous deformation such that there is no self-intersection at any time during the deformation.

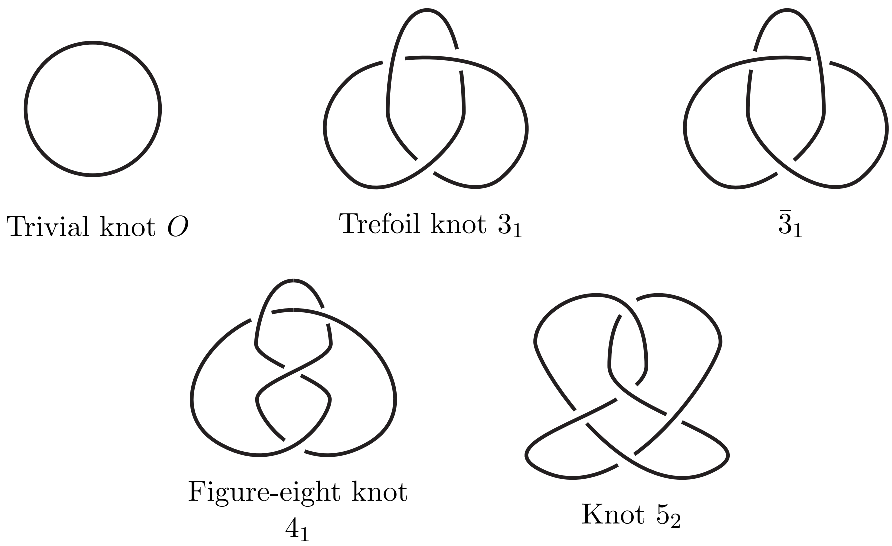

Figure 1.1: Examples of knots.

We present a link on the plane by projecting it into $\mathbb{R}^2$. That image is called a link diagram. A link diagram includes some double points called crossing. Here by deforming a link or a projection we can describe a link diagram such that there is no points such that more than three paths intersect. (See [4])

Theorem 1.1. *Let K and K' be two knots (or two links) and D and D' be their diagrams. Then, K is isotopic to K' if and only if D is obtained from D' by a sequence of isotopies of $\mathbb{R}^2$, and the Reidemeister moves RI, RII and RIII as illustrated in Figure 1.2.*

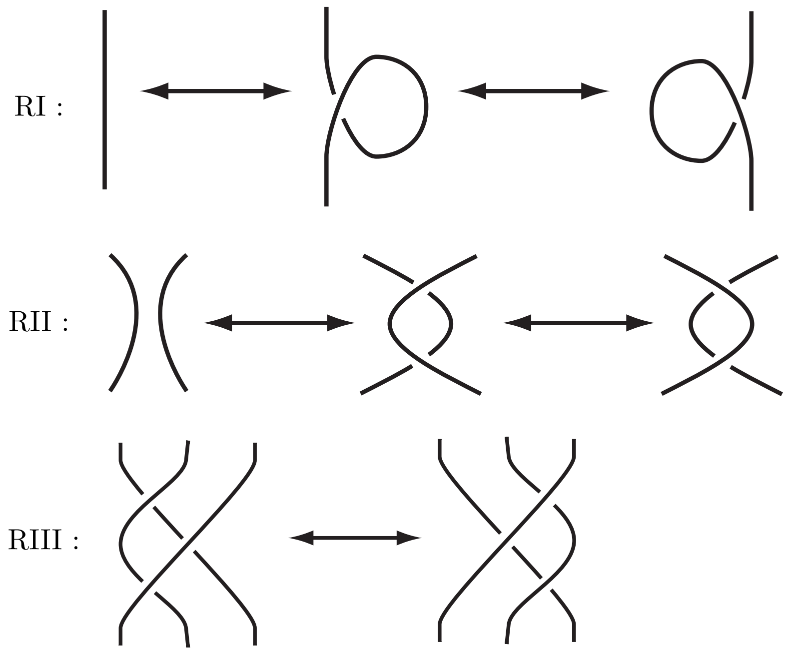

Figure 1.2: Reidemeister moves.

In knot theory we regard isotopic knots as the same object, equivalently we regard diagrams obtained by a sequence of Reidemeister moves as the same object. We want to classify knots or to decide whether given two knots are isotopic or not. It is rather easy to prove two knots are isotopic, because we show a sequence of Reidemeister moves. But it is not easy to prove two knots are not isotopic. To do that it is convenient to use an invariant of knots and links as well as we prove two topological spaces are not homotopic by using their homology groups or fundamental groups.

There are many invariants of knots and links. For example, the fundamental group of the complement of a knot in three-sphere is an invariant. The fundamental group is easy to compute, but it is not usually easy to distinguish knots. We will see another example. The smallest number of crossing changes required to obtain the trivial knot is the invariant called an unknotting number. The unknotting number is easy to define, but not easy to compute, because we must prove the number of crossing changes is minimal.

We consider the polynomial invariants of knots that we associate a knot or a link with a polynomial such that the polynomial is invariant under isotopies or Reidemeister moves.

We will see some examples.

First example is the Alexander polynomial $\Delta_K(t)$ of a knot K. The Alexander polynomial is defined by using the homology group of infinite cyclic cover of the complement of a knot in three-sphere. Equivarentlly we can define the Alexander polynomial as a quantum invariant. The Alexander polynomial satisfy some skein relation and we can easily compute the Alexander polynomial by using this skein relation. The Alexander polynomials of knots in figure 1.1 are as follows.

$$\begin{aligned}
\Delta_O(t) &= 1 \\
\Delta_{3_1}(t) &= t^{-1} - 1 + t = \Delta_{\bar{3}_1}(t) \\
\Delta_{4_1}(t) &= t^{-1} - 3 + t \\
\Delta_{5_2}(t) &= 2t^{-1} - 3 + 2t
\end{aligned}$$

Since $\Delta_{3_1}(t) \neq \Delta_{4_1}(t)$ we conclude that the knot 3_1 is not isotopic to the knot 4_1. We note that the Alexander polynomial is invariant under the mirror image of a knot. But the knot is not usually isotopic with its mirror image. For example the knot 3_1 is not isotopic with it's mirror image $\bar{3}_1$. To distinguish knots which we can not distinguish by the Alexander polynomial, we need more stronger invariants of knots.

Next example is the Jones polynomial. This invariant is introduced by Jones using the theory of operator algebras [16]. Here is some examples of the Jones polynomial.

$$\begin{aligned}
V_O(t) &= 1 \\
V_{3_1}(t) &= -t^{-4} + t^{-3} + t^{-1} \\
V_{\bar{3}_1}(t) &= t + t^3 - t^4 \\
V_{4_1}(t) &= t^{-2} - t^{-1} + 1 + t + t^2 \\
V_{5_2}(t) &= t^{-1} - t^{-2} + 2t^{-3} - t^{-4} + t^{-5} - t^{-6}
\end{aligned}$$

Since $V_{3_1}(t) \neq V_{\bar{3}_1}(t)$ we conclude that the knot 3_1 is not isotopic to its mirror image $\bar{3}_1$. So the Jones polynomial is stronger than the Alexander polynomial. But we do not know the geometric interpretation of the Jones polynomial completely.

In the next section we define the Alexander polynomial and the Jones polynomial as quantum invariants. There are many stronger invariants than the Jones polynomial in quantum invariants but it may be not usually easy to compute. Also we do not knot the geometric interpretation of quantum invariants.

1.2 Quantum invariants of knots

In this section, we review how to construct quantum invariants as operator invariants of oriented tangles following [31].

An oriented tangle is a compact 1-dimensional manifold with orientations in $\mathbb{R} \times \mathbb{R} \times [0, 1]$ whose end points are in $\{0\} \times \mathbb{R} \times \{0, 1\}$. Two tangles are isotopic if one is obtained from the other by an isotopy in $\mathbb{R}^2 \times [0, 1]$ which fixes end points of tangles and preserves orientations. If the tangle has m points of its boundary in $\{0\} \times \mathbb{R} \times \{1\}$ and n points of its boundary in $\{0\} \times \mathbb{R} \times \{0\}$, then we call it an (m, n)-tangle. Thus, a link is a $(0, 0)$-tangle, and a tangle consists of a link together with a collection of proper arcs.

As a knot diagram we present a tangle in the plane by projecting to $\mathbb{R}\times[0, 1]$ such that there are only double crossings and no tangency. We call it a tangle diagram. Let T and T' be two oriented tangles and D and D' be their tangle diagrams. Then, T is isotopic to T' if and only if D is obtained from D' by a sequence of isotopies of $\mathbb{R} \times [0, 1]$ which fix end points, and the Reidemeister moves RI, RII and RIII (with all possible orientations) and moves (with all possible orientations) as illustrated in Figure 1.3.

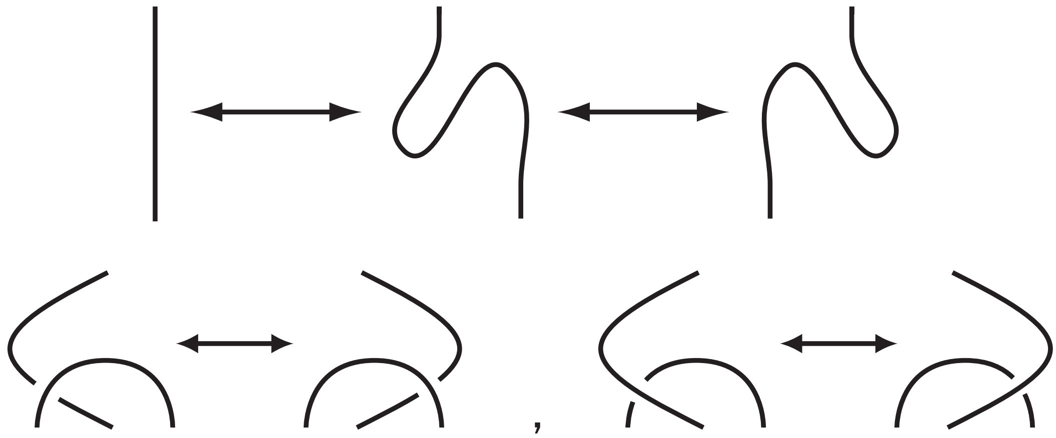

Figure 1.3: Local moves for tangles

Let V be a vector space over $\mathbb{C}$ and V^* be its dual vector space. To associate an oriented tangle diagram D with some linear map we slice D by horizontal lines such that each domain between adjacent horizontal lines is the tangle called elementary tangle which includes either single crossing or single local maximal point or single local minimal point. We associate V to each point where the tangle passes downward a horizontal line and V^* to each point the tangle passes upward a horizontal line, and we take the tensor product along each horizontal line. Here we associate $\mathbb{C}$ to the horizontal line which does not intersect the tangle. Further, we associate linear maps to each elementary tangle as in Figure 1.4.

Here we consider two invertible endomorphisms $R \in \mathrm{End}(V \otimes V)$ and $h \in \mathrm{End}(V)$. The maps n and n' are defined by $n(x \otimes f) = f(hx)$ and $n'(x \otimes f) = f(x)$ for $x \in V$ and $f \in V^*$. The maps u and u' are defined by $u(1) = \sum_i {e_i}^* \otimes (h^{-1}e_i)$ and $u'(1) = \sum_i e_i \otimes {e_i}^*$ where $\{e_i\}$ is a basis of V and $\{{e_i}^*\}$ is the dual basis to $\{e_i\}$. Then we associate a tangle diagram to a linear map by the composition of tensor products the linear maps as in Figure 1.5

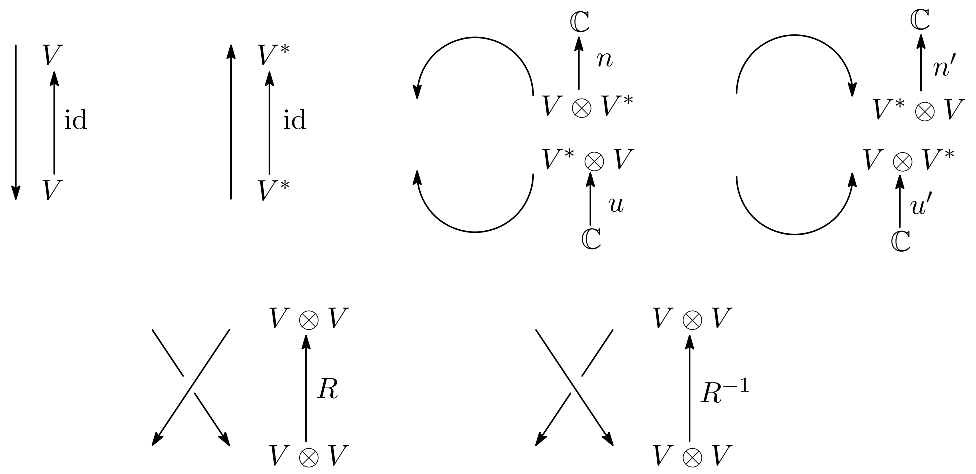

Figure 1.4: The linear maps associated to elementary tangles.

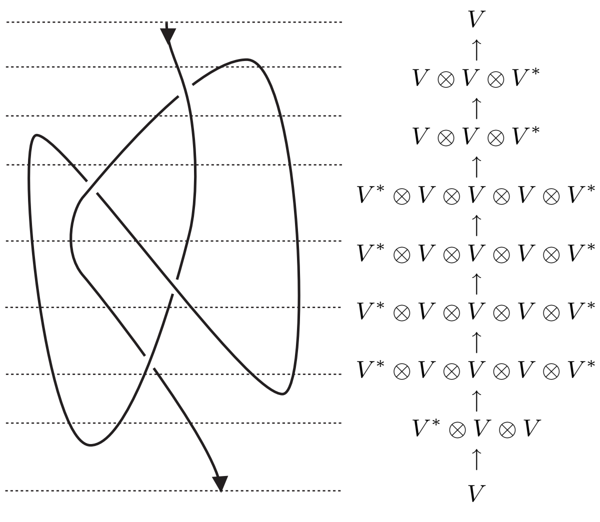

Figure 1.5: The tangle diagram and the linear map

We must define R and h such that this linear map is an isotopy invariant of tangle. the necessary condition is following Theorem due to V. Turaev, P. Freed and D. Yetter.

Theorem 1.2. *If $R \in \mathrm{End}(V \otimes V)$ and $h \in \mathrm{End}(V)$ satisfy the following relations,*

$$R \circ (h \otimes h) = (h \otimes h) \circ R, \tag{1.1}$$

$$\mathrm{trace}_2 \left((\mathrm{id} \otimes h) \circ R^{\pm 1}\right) = \mathrm{id}, \tag{1.2}$$

$$\begin{aligned}&(n' \otimes \mathrm{id}_{V \otimes V^*}) \circ (\mathrm{id}_{V^*} \otimes R^{-1} \otimes \mathrm{id}_{V^*}) \circ (\mathrm{id}_{V^* \otimes V} \otimes u') \\ &\quad \circ (\mathrm{id}_{V^* \otimes V} \circ n) \circ (\mathrm{id}_{V^*} \otimes R \otimes \mathrm{id}_{V^*}) \circ (u \otimes \mathrm{id}_{V \otimes V^*}) = \mathrm{id}_{V \otimes V^*}\end{aligned} \tag{1.3}$$

$$(R \otimes \mathrm{id}) \circ (\mathrm{id} \otimes R) \circ (R \otimes \mathrm{id}) = (\mathrm{id} \otimes R) \circ (R \otimes \mathrm{id}) \circ (\mathrm{id} \otimes R), \tag{1.4}$$

then the linear map associated the diagram is an isotopy invariant of the tangle.

Note that the relation (1.1) is corresponding to the first figure in Figure 1.3 and the relation (1.2) is corresponding to the Reidemeister move I and the relation (1.3) is corresponding to the second figure in Figure 1.3 and the relation (1.4) is corresponding to the Reidemeister move III. The relation (1.4) is called the Yang-Baxter equation and the solution of the Yang-Baxter equation is called R-matrix. Remark that for Lie algebra we can find R and h satisfying equations (1.1), (1.2), (1.3) and (1.4). (See [12])

We will see some examples of link invariants constructed by the above method.

Example 1.1 (Alexander polynomial)**.** The Alexander polynomial of a link L is obtained from the homology group of the infinite cyclic cover of $S^3 - L$. But we can also define the Alexander polynomial by using linear maps R and h as follows.

Let V be 2-dimensional vector space with a basis $\{e_0, e_1\}$. We define $R \in \mathrm{End}(V \otimes V)$ and $h \in \mathrm{End}(V)$ by

$$R = \begin{pmatrix} t^{-\frac{1}{2}} & 0 & 0 & 0 \\ 0 & 0 & 1 & 0 \\ 0 & 1 & t^{-\frac{1}{2}} - t^{\frac{1}{2}} & 0 \\ 0 & 0 & 0 & -t^{\frac{1}{2}} \end{pmatrix}, \qquad h = \begin{pmatrix} t^{\frac{1}{2}} & 0 \\ 0 & -t^{\frac{1}{2}} \end{pmatrix},$$

with a complex parameter t. Here we present R by a matrix (R^{ij}_{kl}) such that $R(e_k \otimes e_l) = \sum_{i,j} R^{ij}_{kl} e_i \otimes e_j$.

Let L be a link and D be $(1,1)$-tangle diagram obtained by cutting a point of L. Using R and h we obtain a linear map $[D]$ from D. Then $[D]$ determines the scaler map

$$[D] = c \times \mathrm{id}_V,$$

with some scalar c. Moreover this scalar c is equal to the Alexander polynomial $\Delta_L(t)$ of L. This result is a conclusion of the fact that $[D]$ is an intertwiner with respect to the action of the quantum group $U_q(sl_2)$ on an irreducible representation V.

Example 1.2 (Jones polynomial)**.** Let V be a 2-dimensional vector space. We put

$R \in \mathrm{End}(V \otimes V)$ and $h \in \mathrm{End}(V)$ by

$$R = \begin{pmatrix} t^{\frac{1}{2}} & 0 & 0 & 0 \\ 0 & 0 & t & 0 \\ 0 & t & t^{\frac{1}{2}} - t^{\frac{3}{2}} & 0 \\ 0 & 0 & 0 & t^{\frac{1}{2}} \end{pmatrix}, \qquad h = \begin{pmatrix} t^{-\frac{1}{2}} & 0 \\ 0 & t^{\frac{1}{2}} \end{pmatrix},$$

with a complex parameter t. We remark that R and h are obtained from the 2-dimensional irreducible representation of the quantum group $U_t(sl_2)$.

We obtain the linear map $\mathbb{C} \to \mathbb{C}$ obtained from a link L by R and h and the image of this map at 1 is equal to the Jones polynomial of L. Moreover the linear map $V \to V$ obtained from the $(1,1)$-tangle presentation of L determines the scalar map and that scalar is equal to the Jones polynomial normarized such that the value of the trivial knot is 1.

Example 1.3 (Colored Jones polynomial)**.** As a generalization of the Jones polynomial we obtain the colored Jones polynomial as follows. We consider N-dimensional irreducible representation of the quantum group $U_q(sl_2)$ and we can obtain linear maps R and h by using the universal R-matrix for $U_q(sl_2)$. Let V be an N-dimensional vector space with a basis $\{e_0, e_1, \ldots, e_{N-1}\}$. Then we define R and h by

$$\begin{aligned} R^{ij}_{kl} &= \sum_{n=0}^{\min\{j,N-1-j\}} \delta_{l,i+n}\delta_{k,j-n}\,(-1)^n \frac{(q)_{i+n}(q)_{N-1+n-j}}{(q)_n(q)_i(q)_{N-1-j}} \\ &\qquad\qquad \times q^{-\frac{n^2}{2}-n\left(\frac{N}{2}+i-j\right)+\left(i-\frac{N-1}{2}\right)\left(j-\frac{N-1}{2}\right)}, \\ (R^{-1})^{ij}_{kl} &= \sum_{n=0}^{\min\{i,N-1-i\}} \delta_{l,i-n}\delta_{k,j+n} \frac{(q)_{j+n}(q)_{N-1+n-i}}{(q)_n(q)_j(q)_{N-1-i}} \\ &\qquad\qquad \times q^{-\frac{N-1}{2}n-\left(i-\frac{N-1}{2}\right)\left(j-\frac{N-1}{2}\right)}, \\ h^i_j &= \delta_{i,j} q^{i-\frac{N-1}{2}}, \end{aligned}$$

where h is presented by a matrix $\{h^i_j\}$ such that $h(e_j) = \sum_i h^i_j e_i$ and $(q)_n = \prod_k^n (1-q^k)$. For (1,1)-tangle we obtain the map $V \to V$ and this map is represented by $c\mathrm{id}_V$ with some scalar. We define the colored Jones polynomial $J_N(L;q)$ of a link L by this scalar. Remark that this invariant is normalized such that the value at the trivial knot is 1.

Example 1.4 (Kashaev's invariant)**.** Kashaev's invariant is defined by following R matrix.

$$\begin{aligned} R^{ij}_{kl} &= \theta^{ij}_{kl} \frac{N\,q^{-\frac{1}{2}-(k-j)(i-l+1)}}{(\bar{q})_{[i-j]}(q)_{[j-l]}(\bar{q})_{[l-k-1]}(q)_{[k-i]}}, \\ (R^{-1})^{ij}_{kl} &= \theta^{ij}_{kl} \frac{N\,q^{\frac{1}{2}+(i-l)(k-j+1)}}{(q)_{[i-j]}(\bar{q})_{[j-l]}(q)_{[l-k-1]}(\bar{q})_{[k-i]}}, \end{aligned}$$

where $q = \exp(2\pi\sqrt{-1}/N)$, $\bar{q} = q^{-1}$, $[i] = i(\mathrm{mod}\ N)$, $(x)_{[i]} = (1-x)(1-x^2)\dots(1-x^{[i]})$ and θ^{ij}_{kl} is defined as follows.

$$\theta^{ij}_{kl} = \begin{cases} 1 & \text{if } [i-j]+[j-l]+[l-k-1]+[k-i] = N-1, \\ 0 & \text{otherwise.} \end{cases}$$

This R matrix was constructed from the 6j-symbol for the minimal cyclic representation of the quantum group $\mathcal{U}_q(sl_2)$. In [25] it is proved that this R matrix is equivalent to the R matrix for the colored Jones polynomial.

1.3 Some calculations of colored Jones polynomials

In this section, we will see some examples of the colored Jones polynomials.

Example 1.5. The case of 5_2. We associate following (1,1)-tangle as in Figure 1.6 obtained from 5_2 with the linear map $V \to V$, where V is the N-dimensional irreducible representation of $U_q(sl_2)$.

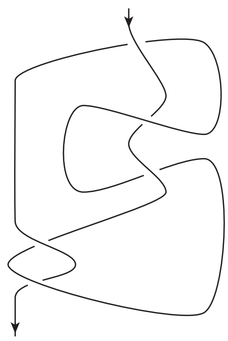

Figure 1.6: (1,1)-tangle presentation of 5_2.

We have

$$\begin{aligned}
V &\xrightarrow{\mathrm{id}\otimes u'} V\otimes V\otimes V \xrightarrow{R^{-1}\otimes\mathrm{id}} V\otimes V\otimes V \xrightarrow{R^{-1}\otimes\mathrm{id}} V\otimes V\otimes V \\
&\xrightarrow{\mathrm{id}\otimes u\otimes\mathrm{id}\otimes\mathrm{id}} V\otimes V\otimes V\otimes V\otimes V \xrightarrow{\mathrm{id}\otimes\mathrm{id}\otimes R^{-1}\otimes\mathrm{id}} V\otimes V\otimes V\otimes V\otimes V \xrightarrow{\mathrm{id}\otimes\mathrm{id}\otimes\mathrm{id}\otimes n} V\otimes V\otimes V \\
&\xrightarrow{\mathrm{id}\otimes\mathrm{id}\otimes\mathrm{id}\otimes u'} V\otimes V\otimes V\otimes V\otimes V \xrightarrow{\mathrm{id}\otimes\mathrm{id}\otimes R^{-1}\otimes\mathrm{id}} V\otimes V\otimes V\otimes V\otimes V \xrightarrow{\mathrm{id}\otimes n'\mathrm{id}\otimes\mathrm{id}\otimes\mathrm{id}} V\otimes V\otimes V \\
&\xrightarrow{R^{-1}\otimes\mathrm{id}} V\otimes V\otimes V \xrightarrow{\mathrm{id}\otimes n} V
\end{aligned}$$

We have the image of this map at the base e_0 as follows.

$$e_0 \to \left(\sum_{i_1,i_2,i_3,i_4,i_5,i_6,i_7,i_8,i_9} (R^{-1})^{i_0 i_8}_{i_4 i_9} (R^{-1})^{i_6 i_9}_{i_7 i_8} (R^{-1})^{i_7 i_1}_{i_6 i_5} (R^{-1})^{i_4 i_5}_{i_2 i_3} (R^{-1})^{i_2 i_3}_{0 i_1} h^{i_8} \right) e_{i_0}$$

So we have the colored Jones polynomial of 5_2 as follows.

$$J_N(5_2, q) = \sum_{i,j,k} (-1)^j \frac{((q)_i)^2 (q)_k}{((q^{-1})_j)^2 (q^{-1})_{i-k} (q)_{k-j}} \, q^{-\frac{5}{4}N^2 - i^2 - \frac{j^2}{2} - ij - 2i - j + k - \frac{3}{4}}.$$

Next, we consider the Whitehead link W.

Example 1.6. We present the Whitehead link as following (1,1)-tangle.

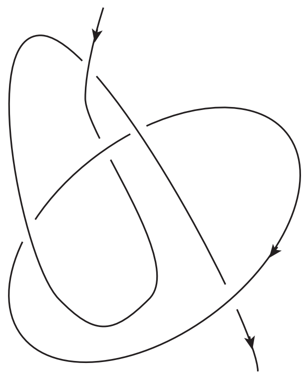

Figure 1.7: (1,1)-tangle presentation of the Whitehead link.

Then the colored Jones polynomial of the Whitehead link is as follows.

$$\begin{aligned} J_N(W; q) &= \sum_{k \le j \le i} (-1)^k \frac{(q)_i (q)_{N-1+j-i} (q)_{N-1}}{(q)_{i-j} (q)_{j-k} (q)_k (q)_{N-1-i} (q)_{N-1-j}} q^{ij+i-jN+\frac{k}{2}(k-2j-2N-1)+\frac{N^2}{4}-\frac{N}{2}+\frac{1}{4}} \\ &= \sum_{j \le i} \frac{(q)_i (q)_{N-1+j-i} (q)_{N-1}}{(q)_{i-j} (q)_j (q)_{N-1-i} (q)_{N-1-j}} \prod_{k=1}^{j} \left(1 - q^{-N-k}\right) q^{ij+i-jN+\frac{N^2}{4}-\frac{N}{2}+\frac{1}{4}} \end{aligned}$$

Here the second equality is followed by the next formula introduced in [25].

$$\sum_{i=0}^{\alpha} (-1)^i q^{\frac{i}{2}(i-\alpha+\beta)} \frac{(q)_\alpha}{(q)_i (q)_{\alpha-i}} = \prod_{k=1}^{\alpha} \left(1 - q^{\frac{\alpha+\beta+1}{2}-k}\right). \tag{1.5}$$

This formula is proved as follows. Set the left hand side of (1.5) be $S(\alpha, \beta)$. We can easily have the following formula.

$$\frac{(q)_n}{(q)_i (q)_{n-i}} = \frac{(q)_{n-1}}{(q)_{i-1} (q)_{n-i}} + q^i \frac{(q)_{n-1}}{(q)_i (q)_{n-i-1}}.$$

Then we have

$$\begin{aligned} S(\alpha, \beta) &= \sum_{i=1}^{\alpha} (-1)^i q^{\frac{i}{2}(i-\alpha+\beta)} \frac{(q)_{\alpha-1}}{(q)_{i-1} (q)_{\alpha-i}} + \sum_{i=0}^{\alpha-1} (-1)^i q^{\frac{i}{2}(i-\alpha+\beta+2)} \frac{(q)_{\alpha-1}}{(q)_i (q)_{\alpha-i-1}} \\ &= (-q^{\frac{1-\alpha+\beta}{2}} + 1) S(\alpha - 1, \beta + 1) \end{aligned}$$

Since $S(0, \beta + \alpha) = 1$ we have the formula (1.5) by induction.

1.4 Volume conjecture

Let $\langle L\rangle_N$ be Kashaev's link invariant associated an positive integer N. This invariant is obtained from the study of the quantum dilogarithm. In [10] R. Kashaev gave following conjecture.

Conjecture 1.1. *For any hyperbolic link L,*

$$\mathrm{Vol}(S^3 - L) = 2\pi \lim_{N\to\infty} \frac{\log|\langle L\rangle_N|}{N},$$

where $\mathrm{Vol}(S^3-L)$ is the hyperbolic volume of S^3-L.

In [10] Kashaev analyzed the asymptotic behavior of his link invariants as the following example.

Example 1.7. Kashaev's invariant of the knot 5_2 denoted by $\langle 5_2\rangle_N$ is described as

$$\langle 5_2\rangle_N = \sum_{k\leq l}^{N-1} \frac{(q)_l^2}{(\bar{q})_k} q^{-k(l+1)},$$

where $q = \exp\left(\frac{2\pi\sqrt{-1}}{N}\right)$, and $(x)_n = \prod_{i=1}^{n}(1-x^i)$. First we consider the integral representation of this summation. Let $S_\gamma(\zeta)$ be the following function

$$S_\gamma(\zeta) = \exp\left(\frac{1}{4}\int_{C(R)} \frac{e^{\zeta z}}{\sinh(\pi z)\sinh(\gamma z) z}\, dz\right),$$

defined on $\{\zeta\in\mathbb{C} \mid |\mathrm{Re}(\zeta)| < \pi+\gamma\}$, where $\gamma\in(0,1)$ and $C(R)$ is the contour $(-\infty,-R)\cup\{R\,e^{(\pi-t)\sqrt{-1}} \mid t\in[0,\pi]\}\cup(R,\infty)$, where $R\in(0,1)$. Here $S_\gamma(\zeta)$ satisfies the following functional equation.

$$(1+e^{\zeta\sqrt{-1}})S_\gamma(\zeta+\gamma) = S_\gamma(\zeta-\gamma).$$

Set $\gamma = \pi/N$ and $N > 3$. By using the above functional equation we can describe $(q)_i$ and $(\bar{q})_i$ as follows.

$$\begin{aligned} (q)_i &= \frac{S_\gamma(\gamma-\pi)}{S_\gamma(-\pi+\gamma+2i\gamma)}, \\ (\bar{q})_i &= \frac{S_\gamma(\pi-\gamma-2i\gamma)}{S_\gamma(\pi-\gamma)} \end{aligned}$$

By applying these formulas we have

$$\begin{aligned} \langle 5_2\rangle_N &= \sum_{k\leq l} \frac{S_\gamma(\gamma-\pi)^2 S_\gamma(\pi-\gamma)}{S_\gamma\left(-\pi+2\pi\left(\frac{l}{N}+\frac{1}{2N}\right)\right)^2 S_\gamma\left(\pi-2\pi\left(\frac{k}{N}+\frac{1}{2N}\right)\right)} \\ &\quad\times \exp\left(-2\pi N\sqrt{-1}\left(\frac{k}{N}\frac{l}{N}\right) - 2\pi\sqrt{-1}\frac{k}{N}\right) \\ &= S_\gamma(\gamma-\pi)^2 S_\gamma(\pi-\gamma)\sum_{k\leq l} f_N\left(\frac{k}{N}+\frac{1}{2N}, \frac{l}{N}+\frac{1}{2N}\right), \end{aligned}$$

where

$$f_N(u,v) = \frac{1}{S_\gamma(-\pi+2\pi u)^2 S_\gamma(\pi-2\pi v)} \times \exp\left(-2\pi N\sqrt{-1}uv - \pi\sqrt{-1}\left(v-u-\frac{1}{2}\right)\right).$$

By using the residue theorem we have

$$\langle 5_2\rangle_N = -\frac{N^2}{4} S_\gamma(\gamma-\pi)^2 S_\gamma(\pi-\gamma)\int_{C_1}\tan(\pi N u)\int_{C(u)}\tan(\pi N v) f_N(u,v)\,dvdu, \quad (1.6)$$

where C_1 is a curve such that the poles $\left\{\frac{l}{N}+\frac{1}{2N} \,\middle|\, l=0,1,\ldots,N-1\right\}$ for $u\to\tan(\pi N u)$ lies inside C_1 and $C(l)$ is a curve such that the poles $\left\{\frac{k}{N}+\frac{1}{2N} \,\middle|\, k=0,1,\ldots,l\right\}$ lies inside $C(l)$. Optimistically we approximate this integral for large N by

$$\langle 5_2\rangle_N \sim -\frac{N^2}{4} S_\gamma(\gamma-\pi)^2 S_\gamma(\pi-\gamma)\int_{C_1}\int_{C(u)} f_N(u,v)\,dvdu. \quad (1.7)$$

Actually we must check this approximation, but in the case of the multi-integral as this this approximation is not justified. In the case of the single integral these justification is discussed in [2].

Now $S_\gamma(\zeta)$ is also described by

$$S_\gamma(\zeta) = \exp\left(\frac{1}{2\gamma\sqrt{-1}}\mathrm{Li}_2(-e^{\zeta\sqrt{-1}}) + I_\gamma(\zeta)\right),$$

where

$$I_\gamma(\zeta) = \frac{1}{4}\int_{C(R)} \frac{e^{\zeta z}}{z\sinh(\pi z)}\left(\frac{1}{\sinh(\gamma z)} - \frac{1}{\gamma z}\right),$$

and $\mathrm{Li}_2(z)$ is Eular's dilogarithm defined by the analytic continuation of the following integral.

$$\mathrm{Li}_2(z) = -\int_0^z \frac{\log(1-t)}{t}dt.$$

Here in [2] they proved the inequality

$$|I_\gamma(\zeta)| \le 2A + B\left(1+e^{-\mathrm{Im}(\zeta)R}\right),$$

where A and B are positive constants only depending on R. By using these equations we approximate (1.7) by

$$\langle 5_2\rangle_N \sim -\frac{N^2}{4} S_\gamma(\gamma-\pi)^2 S_\gamma(\pi-\gamma)\int_{C_1}\int_{C(u)} \exp\frac{N}{2\pi\sqrt{-1}}V(z,w)\,dz\,du,$$

$$V(z,w) = -2\mathrm{Li}_2(z) - \mathrm{Li}_2\left(\frac{1}{w}\right) - \log z\log u + \frac{\pi^2}{2},$$

where we replace q^l and q^k by z and w and ignore the term $\exp\left(-\pi\sqrt{-1}\left(v-u-\frac{1}{2}\right)\right)$. Note that we must check this approximation is valid.

Next we apply the saddle point method to this integral optimistically as follows,

$$\langle 5_2 \rangle \sim M(N) \exp\left(\frac{N}{2\pi\sqrt{-1}} V(z_0, w_0)\right),$$

where $M(N)$ is the function which do not contribute to the large N asymptotics and (z_0, w_0) is one critical point. Here (z_0, w_0) satisfies the following equations.

$$\begin{cases} \exp\left(z\,\dfrac{\partial V}{\partial z}\right) = 1\,, \\ \exp\left(w\,\dfrac{\partial V}{\partial w}\right) = 1\,. \end{cases} \tag{1.8}$$

One solution of (1.8) is

$$(z_0, w_0) = (0.337641 - 0.56228\sqrt{-1}, 0.122561 + 0.744862\sqrt{-1})\,.$$

Then it is numerically confirmed that $\mathrm{Im}(V(z_0, w_0)) = 2.82812208\ldots = \mathrm{Vol}(S^3 - 5_2)$, so we numerically conclude

$$\mathrm{Vol}(S^3 - 5_2) = 2\pi \lim_{N\to\infty} \frac{\log|\langle 5_2\rangle_N|}{N}\,.$$

Note that we must justify the saddle point method for multi-variable cases.

In [39] the ideal triangulation of hyperbolic knots related to Kashaev's invariants was discussed, and it was shown that the equations such as (1.8) derived from Kashaev's invariants coincide with the hyperbolicity equations of the ideal triangulation.

On the other hand, in [25], H. Murakami and J. Murakami proved that Kashaev's link invariant is equal to the colored Jones polynomial evaluated at $\exp\left(\frac{2\pi\sqrt{-1}}{N}\right)$. They extended Kashaev's conjecture to the volume conjecture. Let $J_N(K;q)$ be the colored Jones polynomial of a knot K. Then the volume conjecture is as follows.

Conjecture 1.2 (Volume conjecture)**.** *Let K be a knot in the three-sphere S^3. Then*

$$2\pi \lim_{N\to\infty} \frac{\log|J_N(K;\exp(2\pi\sqrt{-1}/N))|}{N} = v_3||S^3 - K||,$$

where $||S^3 - K||$ is the simplicial volume of $S^3 - K$ and v_3 is the volume of the ideal regular tetrahedron. If K is a hyperbolic knot which means its complement admits the hyperbolic structure, then $v_3||S^3 - K||$ is equal to the hyperbolic volume of $S^3 - K$.

We can formally apply Kashaev's way to analyze asymptotics to the colored Jones polynomial.

Example 1.8. The colored Jones polynomial of the knot 5_2 is described as follows.

$$J_N(5_2) = \sum_{i,j,k} (-1)^j \frac{((q)_i)^2 (q)_k}{((q^{-1})_j)^2 (q^{-1})_{i-k} (q)_{k-j}} \, q^{-\frac{5}{4}N^2 - i^2 - \frac{j^2}{2} - ij - 2i - j + k - \frac{3}{4}} .$$

Here we put $q = \exp\left(\frac{2\pi\sqrt{-1}}{N}\right)$. Next, we formally use following approximations,

$$(q)_i \sim \exp \frac{N}{2\pi\sqrt{-1}} \left(-\mathrm{Li}_2(q^i) + \frac{\pi^2}{6} \right) ,$$

$$(\bar{q})_i \sim \exp \frac{N}{2\pi\sqrt{-1}} \left(\mathrm{Li}_2(q^{-i}) - \frac{\pi^2}{6} \right) ,$$

and applying Kashaev's way we have

$$\begin{aligned} J_N(5_2) \quad &\sim \quad \int \exp \frac{N}{2\pi\sqrt{-1}} V(u,v,w) \, du \, dv \, dw , \\ V(u,v,w) \quad &= \quad -2\mathrm{Li}_2(u) - 2\mathrm{Li}_2\left(\frac{1}{v}\right) - \mathrm{Li}_2\left(\frac{1}{w}\right) - \mathrm{Li}_2\left(\frac{1}{uw}\right) + \mathrm{Li}_2\left(\frac{1}{vw}\right) \\ & \qquad -(\log u)^2 - \frac{(\log v)^2}{2} - \log u \log v + \log(-1) \log v + \frac{5}{6}\pi^2 . \end{aligned}$$

Here we formally put $u = q^i$, $v = q^j$, $w = q^{-k}$. One critical point of $V(u,v,w)$ is

$$(u_0, v_0, w_0) = (0.539798 - 0.182582\sqrt{-1}, 0.122561 + 0.744862\sqrt{-1}, \infty) .$$

Choosing an appropriate branch, the following formula is numerically confirmed.

$$\mathrm{Im}(V(u_0, v_0, w_0)) = \mathrm{Vol}(S^3 - 5_2)$$

In Chapter 2, we discuss the relation between the equations such as the equations such as (1.8) for colored Jones polynomials and the hyperbolicity equations.

We note that the volume conjecture was proved for the figure-eight knot, torus knots and the Borromean rings. But in general this conjecture is not yet proved.

Chapter 2

Hyperbolic geometry and colored Jones polynomials

In this chapter, we discuss the relation between colored Jones polynomials and geometric structures on knot complements.

2.1 Hyperbolic structures on knot complements

In this section, we review how to describe hyperbolic structure on 3-manifolds from it's ideal triangulation due to W. Thurston [36]. (See also [3] and [32])

The hyperbolic 3-space $\mathbb{H}^3$ is the upper half space

$$\{(x_1, x_2, x_3) \in \mathbb{R}^3 \,|\, x_3 > 0\}$$

equipped with the metric defined by

$$ds^2 = \frac{dx_1{}^2 + dx_2{}^2 + dx_3{}^2}{x_3}.$$

Geodesics in $\mathbb{H}^3$ are straight-lines and semi-circles orthogonal to the sphere at infinity $\{(x_1, x_2, 0) \in \mathbb{R}^3\} \cup \{\infty\} \cong \mathbb{C} \cup \{\infty\}$ denoted by S_∞. It is known that the group of isometries of the hyperbolic 3-space denoted by $\mathrm{Isom}(\mathbb{H}^3)$ is isomorphic to $\mathrm{PSL}(2;\mathbb{C}) = SL(2;\mathbb{C})/\{\pm I\}$.

A hyperbolic structure on a 3-manifold M is a Riemannian metric on M such that every point in M has a neighbourhood isometric to an open subset of hyperbolic 3-space.

Let Γ be a discrete, torsion-free subgroup of the group of isometries of $\mathbb{H}^3$. Then Γ acts discontinuously and freely on $\mathbb{H}^3$ and $\mathbb{H}^3/\Gamma$ admits a hyperbolic structure. In general there is a homomorphism of $\pi_1(M)$ into $\mathrm{Isom}(\mathbb{H}^3)$. This homomorphism is called the holonomy representation associated to the hyperbolic structure and defined up to conjugacy.

An ideal tetrahedron in $\mathbb{H}^3$ is a tetrahedron all of whose vertices lie on S_∞ and all of whose edges are geodesics. (Figure 2.1)

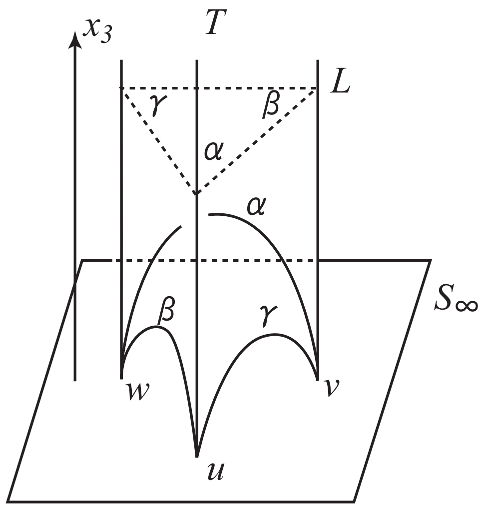

Figure 2.1: The ideal tetrahedron T and its horospherical cross-section $L(v)$.

An ideal tetrahedron is determined up to isometry by the dihedral angle α, β and γ, or equivalently the Euclidean triangle L obtained by cutting out by the horospherical cross-section at a vertex. We can put vertices of an ideal tetrahedron at 0, 1, z and ∞ in S_∞ by using isometries. So an ideal tetrahedron is determined by a single complex number z with positive imaginary part and dihedral angles are $\arg z$, $\arg\left(1 - \frac{1}{z}\right)$ and $\arg \frac{1}{1-z}$ as in Figure 2.2.

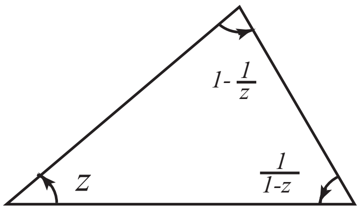

Figure 2.2: Dihedral angles of the ideal tetrahedron determined by a complex number z.

Let M be a 3-manifold obtained by gluing ideal tetrahedra $T_1, \ldots, T_n$ by hyperbolic isometries. Here suppose that each T_i is parametrized by the complex parameter z_i. We can describe a complete hyperbolic structure on M by giving conditions of tetrahedra parameters z_i as follows.

First, we extend a hyperbolic structure on $M - \{\text{1-skeleton}\}$ to M. To do that we consider a neighbourhood of an edge in M. Let $e_1, \ldots, e_n$ be edges in M and $T(j)_i$ be the tetrahedron which has e_i as an edge. Remark that the same tetrahedron may appear more than once between $T(j)_i$'s. We denote the complex parameter of the tetrahedron $T(j)_i$ by $z(i,j) \in \left\{z_k, 1-\frac{1}{z_k}, \frac{1}{1-z_k}\right\}$. The existence of a hyperbolic structure forces triangles to line up neatly around e_i for all i. (Figure 2.3) We call this relation the consistency relation at the edge e_i.

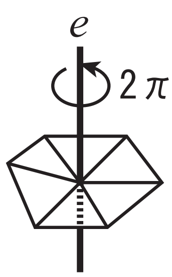

Figure 2.3: Around an edge e.

This condition is given by following algebraic equations for each i.

$$\prod_j z(i,j) = 1, \quad \sum_j \arg z(i,j) = 2\pi.$$

Next, we consider when these ideal tetrahedra give a complete hyperbolic structure on M. We note that near an ideal vertex a complete hyperbolic structure of finite volume has the form (horoball)/$(\mathbb{Z} \oplus \mathbb{Z})$. This means that the horosphere about an ideal vertex equips a Euclidean structure. The ideal triangulation induces the triangulation of the horosphere, and we can describe Euclidean structure on the horosphere by using complex parameters corresponding to ideal tetrahedra.

2.2 Ideal triangulation of 2-bridge link complement

Let L be the 2-bridge link $C(a_1, \ldots, a_n)$ in the Conway such that $n \geq 2, a_i > 0, a_1 \geq 2, a_n \geq 2$. We put $c_0 = 0, c_1 = a_1, c_i = c_{i-1} + a_i$.

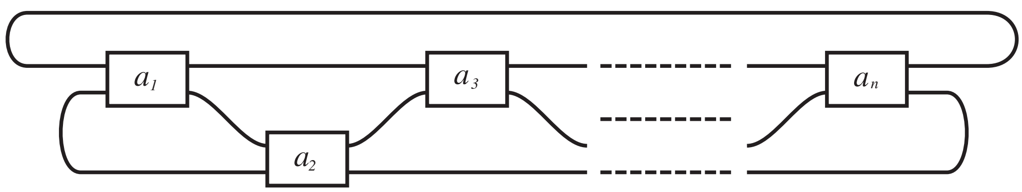

Figure 2.4: 2-bridge link $C(a_1, \ldots, a_n)$.(n is odd)

Here the box labelled a_i denotes the following tangle.

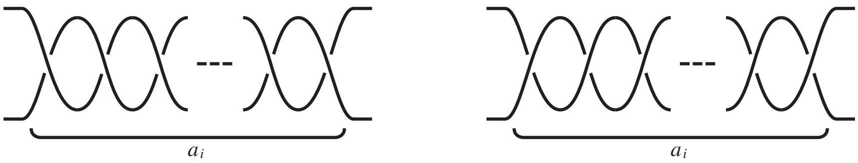

i is odd $\qquad$ i is even

We will decompose $S^3 - L$ into ideal tetrahedra in the same way as [39]. First we put an octahedron $E_iA_iB_iC_iD_iF_i$ at the ith crossing point as illustrated in Figure 2.5 and Figure 2.6, and each octahedron is divided into five tetrahedra.

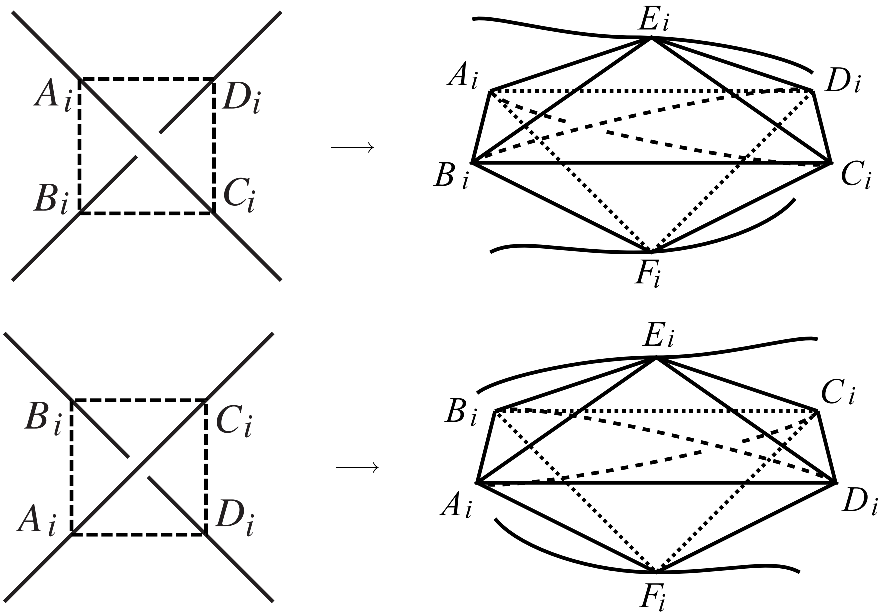

Figure 2.5: The octahedron on ith crossing point.

We put a hyperbolic structure on each tetrahedron by assigning a complex number a_i to the edge E_iA_i of the tetrahedron $E_iA_iB_iD_i$, a complex number b_i to the edge F_iB_i of the tetrahedron $F_iA_iB_iC_i$, a complex number c_i to the edge E_iC_i of the tetrahedron $E_iB_iC_iD_i$, a complex number d_i to the edge F_iD_i of the tetrahedron $F_iA_iC_iD_i$ and a complex number e_i to the edge A_iC_i of the tetrahedron $A_iB_iC_iD_i$. Note that these parameters correspond to q-factorials of the colored Jones polynomial of L. We deform an octahedron attached to the ith crossing point as follows. We pull the vertices B_i and D_i upward and identify the edge E_iB_i with the edge E_iD_i. Similarly we pull the vertices A_i and C_i downward and identify the edge F_iA_i with the edge F_iC_i. If we identify two faces facing each other along an

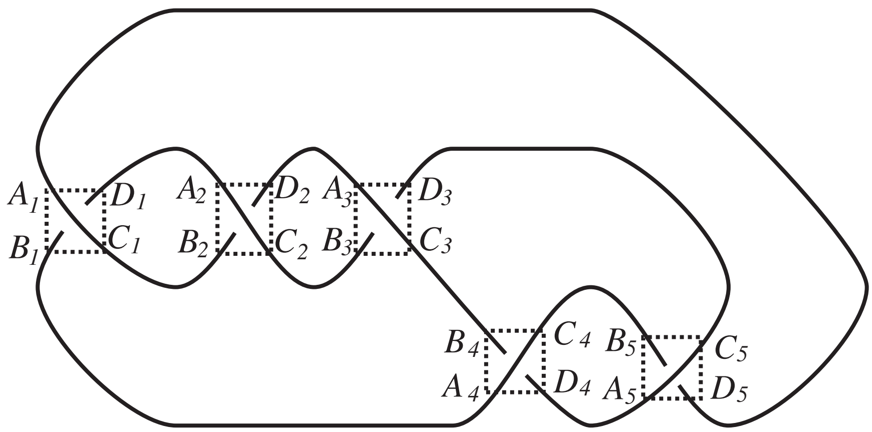

Figure 2.6: Put octahedra at crossings.

arc as illustrated in Figure 2.7, then we have an ideal tetrahedra decomposition of $S^3-(L\cup\{\pm\infty\})$. Here the vertices B_1, D_1, B_2, $D_2,\ldots,B_{c_n}$, D_{c_n} are identified with a vertex $+\infty$, and the vertices A_1, C_1, A_2, $C_2,\ldots,A_{c_n}$, C_{c_n} are identified with a vertex $-\infty$. The vertices E_1, F_1, E_2, $F_2,\ldots,E_{c_n}$, F_{c_n} are identified with one vertex G or two vertices G_1, G_2.

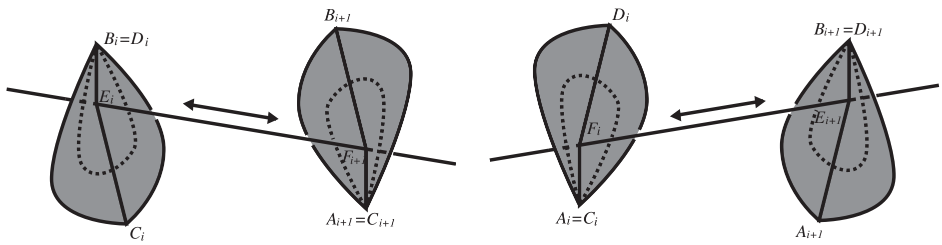

Figure 2.7: Identify two faces facing each other.

Let $N(G)$, $N(G_i)$, $N(+\infty)$ and $N(-\infty)$ be the regular neighbourhood of G, G_i, $+\infty$ and $-\infty$ in S^3. Let $\mathcal{B}$ be the regular neighbourhood of $\triangle E_1A_1B_1\cup\triangle E_1A_1D_1 = \triangle F_{c_n}\ A_{c_n}D_{c_n}\cup\triangle F_{c_n}C_{c_n}D_{c_n}$. If we remove $\mathcal{B}$ from $S^3-N(L\cup\{\pm\infty\})$ then we obtain the ideal triangulation of S^3-L. The first octahedron $E_1A_1B_1C_1D_1F_1$ and the last octahedron $E_{c_n}A_{c_n}B_{c_n}C_{c_n}D_{c_n}\ F_{c_n}$ are essentially 2-dimensional objects in $S^3-(N(L\cup\{\pm\infty\})\cup\mathcal{B})$. Because $\triangle E_1A_1B_1\cup\triangle E_1A_1D_1$ contains the edge A_2D_2 and the edge F_2B_2, the tetrahedron $E_2B_2C_2D_2$ survives in the octahedron $E_2A_2B_2C_2D_2F_2$. Similarly the tetrahedron $F_{c_n-1}A_{c_n-1}B_{c_n-1}C_{c_n-1}$ survives. If $2<i<c_n-1$, $\triangle E_1A_1B_1\cup\triangle E_1A_1D_1$ contains the edge A_iD_i, therefore two tetrahedra $F_iA_iB_iC_i$ and $E_iB_iC_iD_i$ survive in the octahedron $E_iA_iB_iC_iD_iF_i$. So

this ideal triangulation of S^3-L consists of $2(c_n-3)$ tetrahedra. The gluing pattern of $S^3-(L\cup\{\pm\infty\})$ induces the gluing pattern of the ideal triangulation of S^3-L. Figure 2.8 represents the 1-skeleton of the dual complex of this ideal triangulation. Each vertex in Figure 2.8 represents an ideal tetrahedron and the vertex in the i-th row represents tetrahedra at $(i+1)$-th crossing point, and the vertex in the upper column represents the tetrahedron containing E_i, and the vertex in the lower column represents the tetrahedron containing F_i.

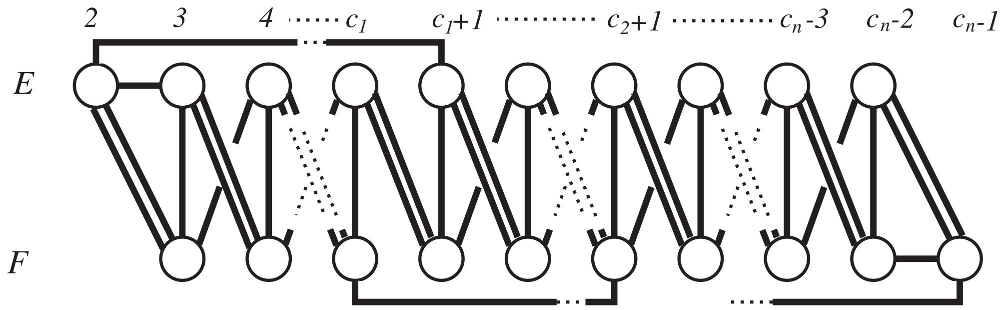

Figure 2.8: The 1-skeleton of the dual complex.

We can see the boundaries of $N(G)$ and $N(\pm\infty)$ as follows. $\partial N(G)$ or $\partial N(G_i)$ is the torus which coincides with the boundary of the regular neighbourhood of one component of the link. The triangulation of $\partial N(G)$induced by the triangulation of $S^3-(L\cup\{\pm\infty\})$ consists of the link of the vertex E_i or the vertex F_i in the octahedron. Each vertical line in Figure 2.9 coincides with the meridian of the boundary of the regular neighbourhood of one component of the link in S^3. $\partial N(+\infty)$ and $\partial N(-\infty)$ are S^2. The triangulation of $S^3-(L\cup\{\pm\infty\})$ induces the triangulation of $\partial N(+\infty)$ and $\partial N(-\infty)$. It is not difficult to draw these triangulation from the link diagram in S^2. We can regard the link diagram as the cell decomposition of S^2. A vertex of the triangulation of $N(+\infty)$ is the 0-cell of the diagram which corresponds to the edge $E_iB_i=E_iD_i$, or the dual 0-cell which corresponds to the edge A_iB_i, the edge B_iC_i, the edge C_iD_i, or the edge A_iD_i, or the crossing point of the link which corresponds to the edge B_iD_i. (Figure 2.10) Similarly a vertex of the triangulation of $N(-\infty)$ is the 0-cell of the diagram which corresponds to the edge $F_iA_i=F_iC_i$, or the dual 0-cell which corresponds to the edge A_iB_i, the edge B_iC_i, the edge C_iD_i, or the edge A_iD_i, or the crossing point which corresponds to the edge A_iC_i. (Figure 2.11)

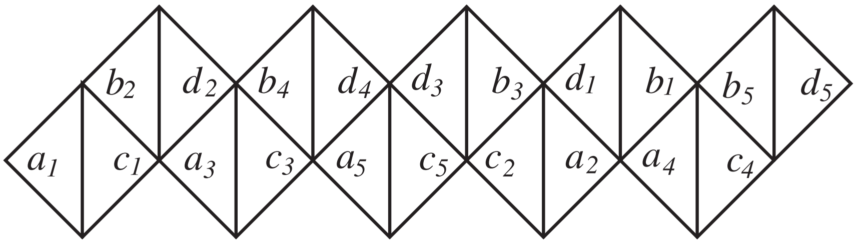

Figure 2.9: The boundary of the regular neighbourhood of G (or G_i).

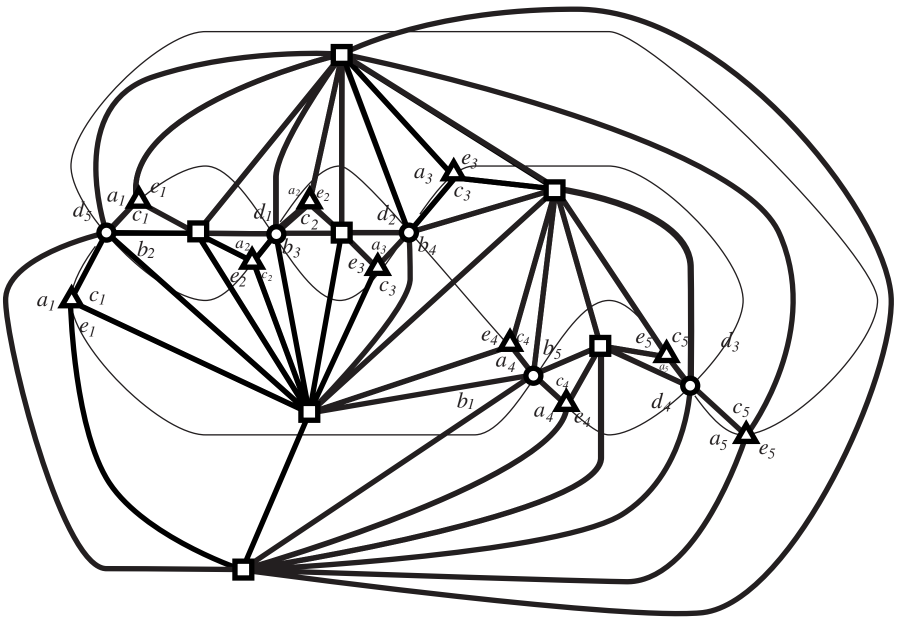

Figure 2.10: The boundary of the regular neighbourhood of $+\infty$. The vertex $\circ$ corresponds to the edge $E_iB_i = E_iD_i$ and the vertex $\square$ in bigonal region corresponds to the edge $C_iD_i = A_{i+1}B_{i+1}$ and the vertex $\square$ in polygonal region corresponds to the edge B_iC_i or the edge A_iD_i and the vertex $\triangle$ corresponds the edge B_iD_i.

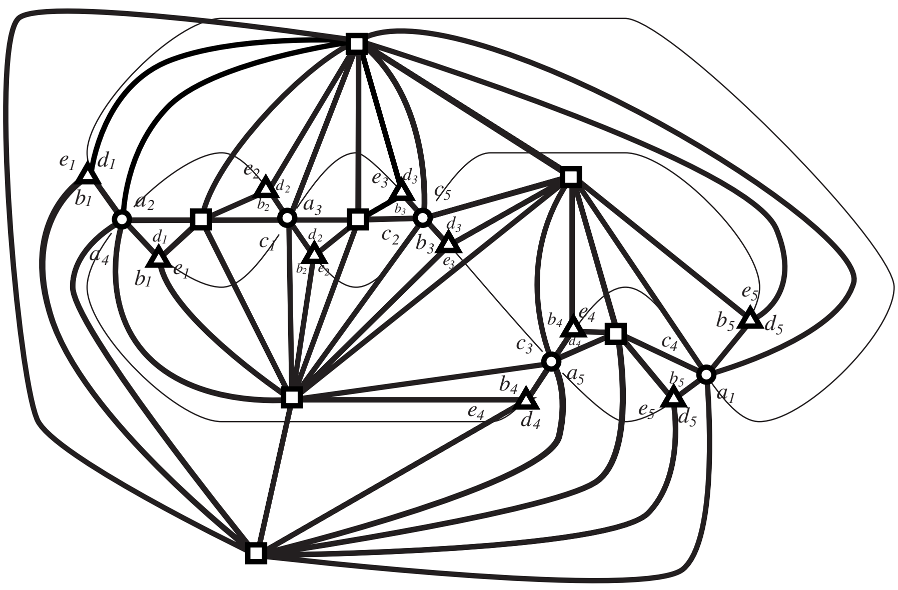

Figure 2.11: The boundary of the regular neighbourhood of $-\infty$. The vertex $\circ$ corresponds to the edge $F_iA_i = F_iC_i$ and the vertex $\square$ in bigonal region corresponds to the edge $C_iD_i = A_{i+1}B_{i+1}$ and the vertex $\square$ in polygonal region corresponds to the edge B_iC_i or the edge A_iD_i and the vertex $\triangle$ corresponds the edge A_iC_i.

We can read the edge relations and the cusp condition from this ideal triangulation of $S^3 - L$ as follows.

First, we can read the edge relations for the edge $E_iB_i = E_iD_i = F_{i+1}B_{i+1}$ and $E_iC_i = F_{i+1}A_{i+1} = F_{i+1}C_{i+1}$ and the cusp condition from the triangulation derived from $\partial N(G)$. Because each vertical line in Figure 2.12 is the meridian of the torus boundary, the cusp condition is

$$b_{i+1} = c_i. \tag{2.1}$$

The edge relation for the edge which contains E_i or F_i is

$$\frac{b_{i+1}}{c_i} = \frac{b_i}{c_{i-1}} \quad \text{or} \quad \frac{b_{i+1}}{c_i} = \frac{c_{i-1}}{b_i}.$$

Here if the cusp condition (2.1) is satisfied then these edge relations is also satisfied. Note that $z_i = b_{i+1} = c_i$ corresponds to the label of a 2-bridge link in the next section.

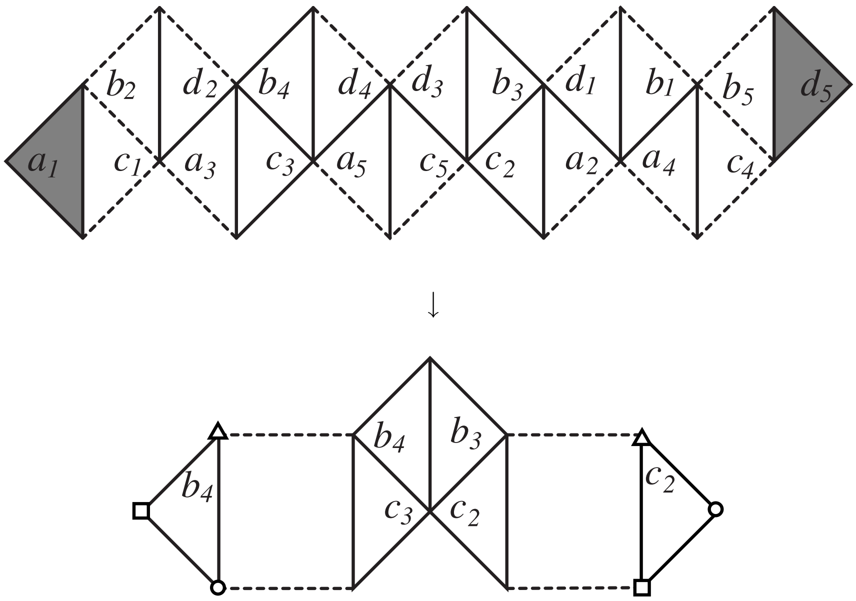

Figure 2.12: The triangulation of $S^3 - L$ derived from $\partial N(G)$. The doted lines are contracted and the left and right triangles in the lower picture belong to the triangulation derived from $\partial N(\pm\infty)$.

The other edge relations are read from the triangulation induced by $\partial N(\pm\infty)$. Each edge relation is the sum of the angle around the vertex corresponding to the dual 0-cell for the polygonal region of the link diagram.

If $c_{m-1} < i < c_m$ and m is odd we can read the edge relation for the edge $C_iD_i = A_{i+1}B_{i+1}$ from Figure 2.13, which corresponds to the vertex $\square$ in Figure 2.13. It is

$$b_i c_{i+1}\left(1-\frac{1}{b_{i+1}}\right)\left(1-\frac{1}{c_i}\right)=1\,. \tag{2.2}$$

Similarly if $c_{m-1} < i < c_m$ and m is even the edge relation for the edge $C_iD_i = A_{i+1}B_{i+1}$ is

$$\frac{b_i c_{i+1}}{(1-b_{i+1})(1-c_i)}=1\,. \tag{2.3}$$

We can read the edge relation for the edge $B_2C_2 = B_3C_3 = \cdots = B_{c_1}C_{c_1} = A_{c_1+1}B_{c_1+1} = E_3B_3 = E_3D_3 = F_4B_4$ from Figure 2.14 and Figure 2.12, which corresponds to the vertex $\square$ in the polygonal region in Figure 2.14. It is

$$c_2 c_{c_1+1}\prod_{j=2}^{c_1}\frac{1}{(1-b_{j+1})(1-c_j)}\left(-\frac{b_4}{c_3}\right)=1\,. \tag{2.4}$$

If m is even we can read the edge relation for the edge $C_{c_m}D_{c_m} = B_{c_m+1}C_{c_m+1} = \cdots = B_{c_{m+1}}C_{c_{m+1}} = A_{c_{m+1}+1}B_{c_{m+1}+1}$ from Figure 2.15.

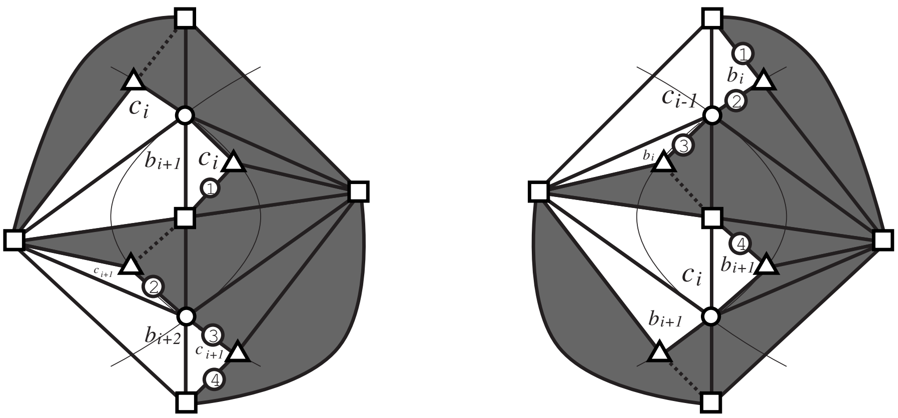

Figure 2.13: The triangulation of $S^3 - L$ derived from $\partial N(\pm\infty)$. This picture is near the dual 0-cell for the bigonal region of the link diagram. The shaded region corresponds to the tetrahedron which is essentially two dimensional object in $S^3 - (N(L \cup \{\pm\infty\}) \cup \mathcal{B})$. The edges with same numbers are identified in the ideal triangulation of $S^3 - L$.

$$b_{c_m} c_{c_{m+1}+1} \prod_{j=c_m}^{c_{m+1}} \frac{1}{(1-b_{j+1})(1-c_j)} = 1\,, \tag{2.5}$$

If m is odd the picture of the triangulation of $\partial N(\pm\infty)$ near the vertex corresponding to the edge $C_{c_m} D_{c_m} = B_{c_m+1} C_{c_m+1} = \cdots = B_{c_{m+1}} C_{c_{m+1}} = A_{c_{m+1}+1} B_{c_{m+1}+1}$ is obtained by reflecting the left and the right figure in Figure 2.15 with respect to a vertical line. So the edge relation for this edge is

$$b_{c_m} c_{c_{m+1}+1} \prod_{j=c_m}^{c_{m+1}} \left(1 - \frac{1}{c_j}\right) \left(1 - \frac{1}{b_{j+1}}\right) = 1\,. \tag{2.6}$$

If n is even the picture of the triangulation of $\partial N(+\infty)$ (respectively $\partial N(-\infty)$) near the vertex corresponding to the edge $C_{c_{n-1}} D_{c_{n-1}} = B_{c_{n-1}+1} C_{c_{n-1}+1} = \cdots = B_{c_n-1} C_{c_n-1} = F_{c_n-2} A_{c_n-2} = F_{c_n-2} C_{c_n-2}$ is obtained by reflecting the right (respectively left) figure in Figure 2.14 with respect to a horizontal line. So the edge relation for this edge is

$$b_{c_{n-1}} c_{c_n-2} \prod_{j=c_{n-1}}^{c_n-2} \left(1 - \frac{1}{b_{j+1}}\right) \left(1 - \frac{1}{c_j}\right) \left(-\frac{c_{c_n-3}}{b_{c_n-2}}\right) = 1\,. \tag{2.7}$$

Similarly if n is odd we can read the edge relation for the edge $C_{c_{n-1}} D_{c_{n-1}} = B_{c_{n-1}+1} C_{c_{n-1}+1} = \cdots = B_{c_n-1} C_{c_n-1} = F_{c_n-2} A_{c_n-2} = F_{c_n-2} C_{c_n-2}$. It is

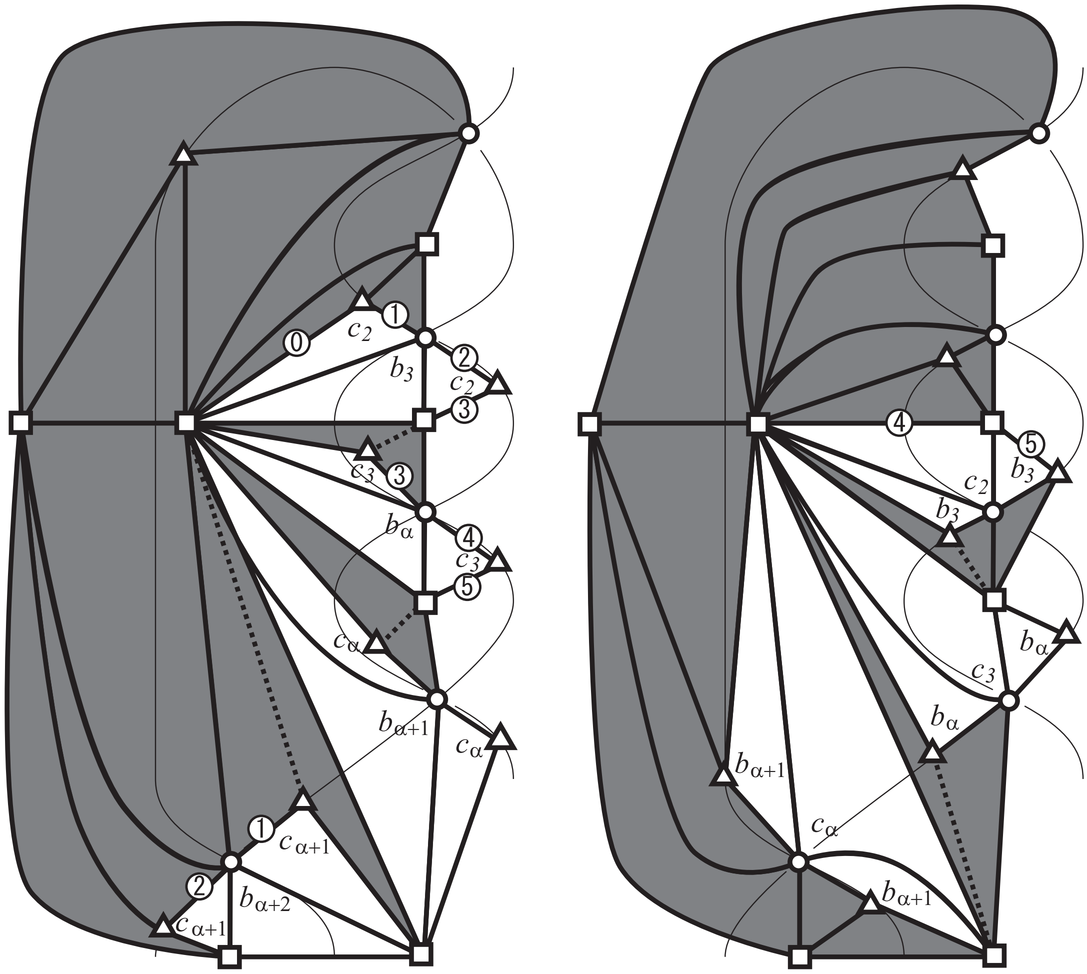

Figure 2.14: The triangulation of $S^3 - L$ derived from $\partial N(\pm\infty)$. This picture is near the dual 0-cell for the first polygonal region. Here $\alpha = c_1$. The doted lines and the shaded regions are contracted and the edges with same numbers are identified in the ideal triangulation. The edge with the number 0 is identified with the boundary of $N(L) - \mathcal{B}$ in the ideal triangulation.

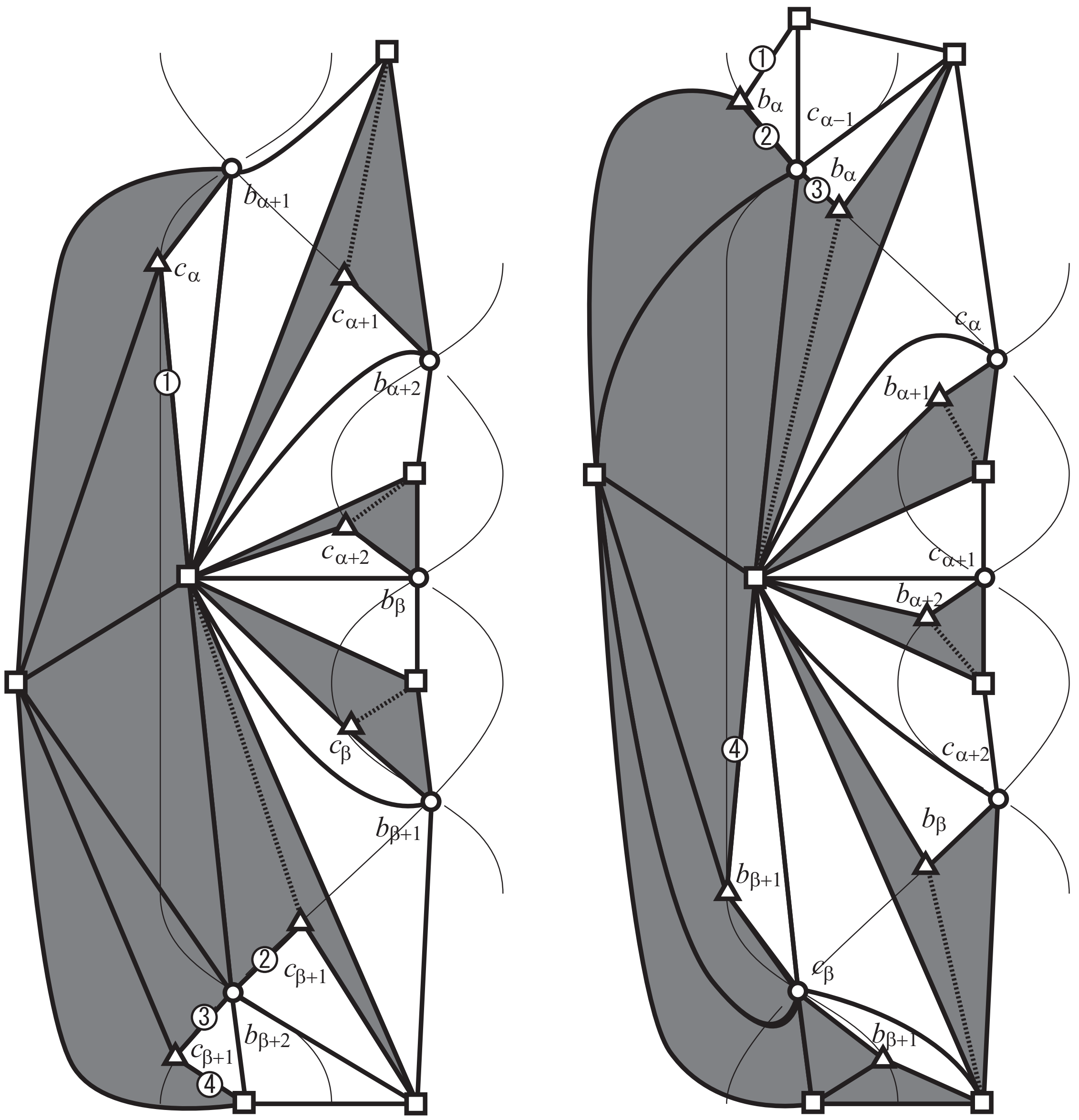

Figure 2.15: The triangulation of $S^3 - L$ derived from $\partial N(\pm\infty)$. This picture is near the dual 0-cell for the polygonal region. Here $\alpha = c_{2m}$ and $\beta = c_{2m+1}$. The doted lines and the shaded regions are contracted and the edges with same numbers are identified in the ideal triangulation.

$$c_{c_{n-1}-1}b_{c_n-1}\prod_{j=c_{n-1}}^{c_n-2}\frac{1}{(1-c_j)(1-b_{j+1})}\left(-\frac{c_{c_n-3}}{b_{c_n-2}}\right)=1\,. \tag{2.8}$$

Now let us consider the complete hyperbolic structure of S^3-L. Because the condition (2.1) is satisfied we can put $z_i=b_{i+1}=c_i$. Then from (2.2) and (2.4) we have

$$\begin{aligned}
1 &= z_2z_{c_1+1}\prod_{j=2}^{c_1}\frac{1}{(1-z_j)^2}(-1)\\
&= -z_2z_{c_1+1}\frac{z_3}{z_2^2}\prod_{j=3}^{c_1-1}\frac{z_{j-1}z_{j+1}}{z_j^2}\,\frac{1}{(1-z_{c_1})^2}\\
&= -\frac{z_{c_1}z_{c_1+1}}{z_{c_1-1}(1-z_{c_1})^2}\,,
\end{aligned}$$

and inductively we have

$$\begin{aligned}
1 &= -\frac{(1-z_{c_m})^2z_{c_m+1}}{z_{c_m-1}z_{c_m}} \quad (m:\text{even})\,,\\
1 &= -\frac{z_{c_m}z_{c_m+1}}{z_{c_m-1}(1-z_{c_m})^2} \quad (m:\text{odd})\,.
\end{aligned}$$

Summarizing above observations the hyperbolicity equations of this ideal triangulation is as follows.

$$\begin{cases}
\left(1-\dfrac{1}{z_j}\right)^2 z_{j-1}z_{j+1}=1 & (c_{2r}<j<c_{2r+1})\,,\\
\dfrac{z_{j-1}z_{j+1}}{(1-z_j)^2}=1 & (c_{2r+1}<j<c_{2r})\,,\\
-\dfrac{z_jz_{j+1}}{(1-z_j)^2z_{j-1}}=1 & (j=c_{2r+1})\,,\\
-\dfrac{(1-z_j)^2z_{j+1}}{z_{j-1}z_j}=1 & (j=c_{2r})\,.
\end{cases} \tag{2.9}$$

Remark. This hyperbolicity equations is equal to the hyperbolicity equations of the canonical decomposition introduced in [34]. But from Figure 2.8 and Figure 2.16 we see that this decomposition is not canonical. On the other hand it is expected that there is the solution $(\zeta_2,\dots,\zeta_{c_n-2})$ of the hyperbolicity equations of the canonical decomposition of a 2-bridge link complement which satisfies $\mathrm{Im}(\zeta_j)>0$. It was shown in [15] that there is such solution if L is a twist knot.

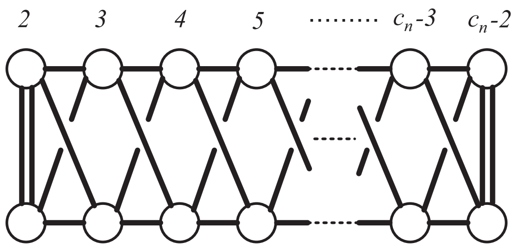

Figure 2.16: The 1-skeleton of the dual complex of canonical decomposition, see [34].

2.3 The colored Jones polynomial of a 2-bridge link

In this section we calculate the N-colored Jones polynomial of a 2-bridge link L evaluated at $q = \exp\left(\frac{2\pi\sqrt{-1}}{N}\right)$ which is denoted by $J_N(L)$ as in [26]. We can calculate $J_N(L)$ in the following way. We present L in a $(1,1)$-tangle D by cutting a component of L. We start with labelling each edge of D with labels $\{0, 1, \ldots, N-1\}$. Here we label the two edges containing the end points by 0. Following the labelling, we associate the positive (respectively negative) crossing with the complex number R^{kl}_{ij} (respectively $(R^{-1})^{kl}_{ij}$) which is $((i,j),(k,l))$-th entry of R-matrix R (respectively R^{-1}), a maximal point labelled by i with the element $q^{-i+\frac{N-1}{2}}$, a minimal point labelled by i with the element $q^{i-\frac{N-1}{2}}$. After multiplying all elements we take summation with all labelings . Here we can label a 2-bridge link L as illustrated in Figure 2.17.

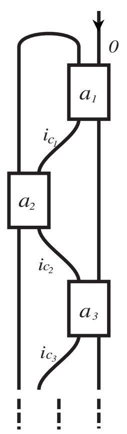

Figure 2.17: Labeling of L.

Here the box labelled a_m in Figure 2.17 denotes the following tangle with labels.

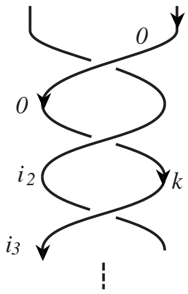

if $m = 1$

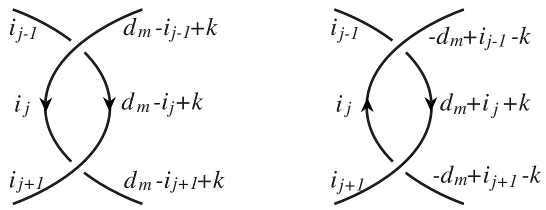

if m is odd

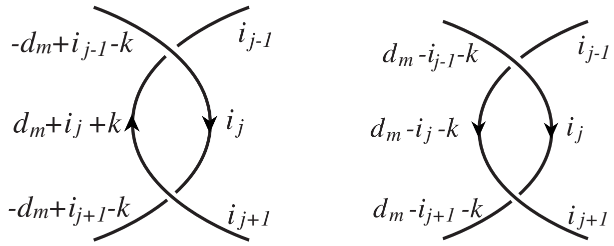

if m is even

Here $d_1 = i_2, d_{m+1} = \pm d_m \pm i_{c_m}$, the sign depends on the orientation of the tangle. For each crossing we assign a complex number as follows.

If $1 \leq c_{m-1} < j < c_m$ and m is odd, we assign the crossing 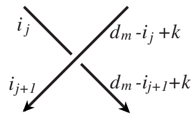

$$(-1)^{i_j+i_{j+1}-N+1} \frac{(q)_{d_m+k-i_j}(q)_{d_m+k-i_{j+1}}}{(q^{-1})_{i_j}(q^{-1})_{i_{j+1}}(q)_{d_m+k-i_j-i_{j+1}}}$$
$$\times q^{-\frac{i_j^2}{2}-\frac{i_{j+1}^2}{2}+i_j i_{j+1}-\frac{N}{2}(i_j-i_{j+1})-\frac{N^2}{4}+\frac{1}{4}}.$$

We assign the crossing 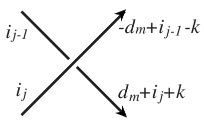

$$(-1)^{i_j+i_{j-1}-N+1} \frac{(q)_{i_j}(q)_{d_m+k+i_j}}{(q^{-1})_{i_{j-1}}(q)_{d_m+k-i_{j-1}+i_j}(q^{-1})_{-d_m-k+i_{j-1}}}$$
$$\times q^{-\frac{i_{j-1}^2}{2}-\frac{i_j^2}{2}-i_{j-1}i_j-i_j-\frac{1}{2}i_{j-1}-\frac{d_m+k}{2}+N\left(1-\frac{d_m+k}{2}+i_{j-1}+i_j\right)-\frac{3N^2}{4}-\frac{1}{4}}.$$

We assign the crossing 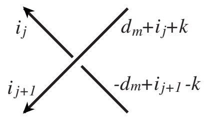

$$(-1)^{i_j+i_{j+1}-N+1}\frac{(q)_{i_j}(q)_{d_m+k+i_j}}{(q^{-1})_{i_{j+1}}(q)_{d_m+k+i_j-i_{j+1}}(q^{-1})_{i_{j+1}-d_m-k}}$$
$$\times q^{-\frac{i_j^2}{2}-\frac{i_{j+1}^2}{2}-i_ji_{j+1}+\frac{d_m+k-i_j-3i_{j+1}}{2}+N\left(\frac{d_m+k}{2}+1+i_j+i_{j+1}\right)-\frac{3N^2}{4}-\frac{1}{4}}.$$

If $c_{m-1}<j<c_m$ and m is even, we assign the crossing 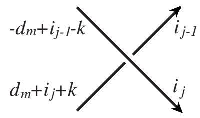

$$\frac{(q)_{i_{j-1}}(q^{-1})_{-d_m-k+i_{j-1}}}{(q^{-1})_{i_j}(q^{-1})_{i_{j-1}-i_j-d_m-k}(q)_{d_m+k+i_j}}$$
$$\times q^{i_{j-1}i_j-\frac{d_m+k}{2}+i_{j-1}+N\left(\frac{d_m+k-1}{2}-i_{j-1}\right)+\frac{N^2}{4}+\frac{1}{4}}.$$

We assign the crossing 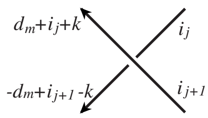

$$\frac{(q)_{i_{j+1}}(q^{-1})_{i_{j+1}-d_m-k}}{(q^{-1})_{i_j}(q)_{d_m+k+i_j}(q^{-1})_{i_{j+1}-i_j-d_m-k}}\,q^{i_ji_{j+1}+\frac{d_m+k}{2}+i_j-N\left(\frac{d_m+k+1}{2}+i_j\right)+\frac{N^2}{4}+\frac{1}{4}}.$$

We assign the crossing 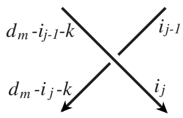

$$\frac{(q^{-1})_{d_m-k-i_{j-1}}(q^{-1})_{d_m-k-i_j}}{(q^{-1})_{i_{j-1}}(q^{-1})_{i_j}(q^{-1})_{d_m-k-i_{j-1}-i_j}}\,q^{-i_{j-1}i_j+\frac{N}{2}(i_{j-1}+i_j+1)-\frac{N^2}{4}-\frac{1}{4}}.$$

From the definition, $J_N(L)$ is the sum of the product of the above quantities, so it is

$$\begin{aligned} J_N(L) &= C\sum_{i_2,i_3,\dots,i_{c_n-2},k}(-1)^{i_{c_1}+\cdots+i_{c_{n-1}}}\prod_{j=2}^{c_n-2}\left((q^{\varepsilon_j})_{i_j}^{\varepsilon_j}\right)^2 \\ &\qquad \prod_S (q^{\varphi_S})_{\varphi_S k+S}^{\varepsilon_S}\times q^P\,, \qquad (2.10)\\ P &= -\sum_{l=1}^{c_n-2}\Big((-1)^l\sum_{c_{l-1}<j\le c_l}\varepsilon_{j-1}\varepsilon_j i_{j-1}i_j-\sum_{\substack{c_{l-1}<j<c_l\\ l:\text{ odd}}} i_j^2-\frac{1}{2}i_{c_l}^2\Big)+T\,. \end{aligned}$$

Here C is constant number, $\varepsilon_j=\pm1,\varepsilon_S=\pm1,\varphi_S=\pm1$, S and T is linear functions of $i_2,\dots,i_{c_n-2}$. Note that each q-factorial $(q)_{i_j}$ corresponds to the tetrahedron parametrized by b_i or c_i which consists of the ideal tetrahedra decomposition of $S^3 - L$, and $(q)_{k+S}$ corresponds to the tetrahedron parametrized by a_i or d_i which is essentially two or one dimensional object in $S^3 - N(L \cup \{\pm\infty\}) - \mathcal{B}$. Put complex parameters $z_2, \dots, z_{c_n - 2}$, and w as follows. If we label the arc 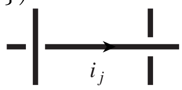 we put $q^{i_j} = z_j$. If we label the arc 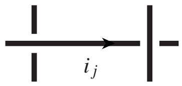 we put $q^{-i_j} = z_j$. And we put $q^k = w^{-1}$.

Applying Kashaev's way we have

$$
\begin{aligned}
&V(z_2, \dots z_{c_1}, \dots z_{c_n - 2}, w) \\
&\quad = -2 \sum_{j=2}^{c_n - 2} \mathrm{Li}_2(z_j) - \sum_{l=1}^{n} \Big(\sum_{\substack{j = c_{l-1}+1 \\ l : \text{odd}}}^{c_l - 1} (\log z_j)^2 + (-1)^l \sum_{j = c_{l-1}+1}^{c_l} (\log z_{j-1} \log z_j) \Big) \\
&\qquad - \frac{1}{2} \sum_{l=1}^{n-1} (\log z_{c_l})^2 + \log(-1) \left(\sum_{l=1}^{n-1} \log z_{c_l} \right) + \sum_A \mathrm{Li}_2(A/w) + \alpha \,,
\end{aligned}
$$

where $A = \prod_j z_j^{\varepsilon_j}$ is determined by S in (2.10) and α is the constant number defined as follows.

$$
\alpha = \begin{cases} \sum_{l=1}^{r-1} \left(a_{2l+1} \dfrac{\pi^2}{2} + a_{2l} \dfrac{\pi^2}{6} \right) + (a_1 - 2)\dfrac{\pi^2}{2} + (a_n - 2)\dfrac{\pi^2}{6} + \dfrac{\pi^2}{3} & (n = 2r) \\ \dfrac{\pi^2}{2} \sum_{l=1}^{r-1} a_{2l+1} + \dfrac{\pi^2}{6} \sum_{l=1}^{r} a_{2l} + (a_1 - 2)\dfrac{\pi^2}{2} + (a_n - 2)\dfrac{\pi^2}{2} + \dfrac{\pi^2}{3} & (n = 2r+1) \end{cases}
$$

Here $w = \infty$ satisfies the equation $\exp\left(w \dfrac{\partial V}{\partial w} \right) = 1$. So the critical point $(z_2, \dots z_{c_n - 2}, \infty)$ satisfies the following equations.

$$
\begin{cases} \left(1 - \dfrac{1}{z_j}\right)^2 z_{j-1} z_{j+1} = 1 & (c_{2r} < j < c_{2r+1}) \,, \\ \dfrac{(1 - z_j)^2}{z_{j-1} z_{j+1}} = 1 & (c_{2r+1} < j < c_{2r}) \,, \\ -\dfrac{(1 - z_j)^2 z_{j-1}}{z_j z_{j+1}} = 1 & (j = c_{2r+1}) \,, \\ -\dfrac{(1 - z_j)^2 z_{j+1}}{z_j z_{j-1}} = 1 & (j = c_{2r}) \,. \end{cases} \tag{2.11}
$$

These equations coincide with (2.9).

If $(\zeta_2, \dots, \zeta_{c_n - 2}, \infty)$ is the solution of (2.11) such that $\mathrm{Im}(\zeta_j) > 0$ $(j = 2, \dots, c_n -$

2), from (2.11) we have

$$\begin{cases} -2\arg\zeta_j + 2\arg(1-\zeta_j) + \arg\zeta_{j-1} + \arg\zeta_{j+1} = 0 & (c_{2r} < j < c_{2r+1})\,, \\ 2\arg(1-\zeta_j) - \arg\zeta_{j-1} - \arg\zeta_{j+1} = 0 & (c_{2r+1} < j < c_{2r+2})\,, \\ \pi - \arg\zeta_j + 2\arg(1-\zeta_j) + \arg\zeta_{j-1} - \arg\zeta_{j+1} = 0 & (j = c_{2r+1})\,, \\ \pi - \arg\zeta_j + 2\arg(1-\zeta_j) - \arg\zeta_{j-1} + \arg\zeta_{j+1} = 0 & (j = c_{2r})\,. \end{cases}$$

The imaginary part of $V(\zeta_2, \ldots \zeta_{c_n-2}, \infty)$ is calculated as follows.

$$\begin{aligned} &\mathrm{Im}(V(\zeta_2, \ldots \zeta_{c_n-2}, \infty)) \\ &= -2\,\mathrm{Im}(\sum_{j=2}^{c_n-2} \mathrm{Li}_2(\zeta_j)) + \sum_r \Big(\sum_{j=c_{2r}+1}^{c_{2r+1}-1} \log|\zeta_j|(-2\arg\zeta_j + \arg\zeta_{j-1} + \arg\zeta_{j+1}) \\ &\quad - \sum_{j=c_{2r+1}}^{c_{2r}-1} \log|\zeta_j|(\arg\zeta_{j-1} + \arg\zeta_{j+1})\Big) \\ &\quad + \sum_{j=c_{2r+1}} \log|\zeta_j|(-\arg\zeta_j + \pi - \arg\zeta_{j-1} + \zeta_{j+1}) \\ &\quad + \sum_{j=c_{2r}} \log|\zeta_j|(-\arg\zeta_j + \pi + \arg\zeta_{j-1} - \zeta_{j+1}) \\ &= -2\sum_{j=2}^{c_n-2} D(\zeta_j)\,. \end{aligned}$$

Here $D(z)$ is the hyperbolic volume of the ideal tetrahedron with parameter z.

$$D(z) = \mathrm{Im}\mathrm{Li}_2(z) + \log|z|\arg(1-z)\,.$$

On the other hand, since $(\zeta_2, \ldots, \zeta_{c_n-2})$ is also the solution of the hyperbolicity equations (2.9), we have

$$\mathrm{Vol}(S^3 - L) = 2\sum_{j=2}^{c_n-2} D(\zeta_j)\,.$$

So we have $\mathrm{Vol}(S^3 - L) = -\mathrm{Im}(V(\zeta_2, \ldots \zeta_{c_n-2}, \infty))$.

Summarizing above observations we have the next Proposition.

Theorem 2.1. *For the alternating 2-bridge link, $V(z_2, \ldots, z_{c_n-2}, w)$ denotes the function obtained from the colored Jones polynomial by Kashaev's way. Then the system of the equations* $\left\{\exp\left(z_j \dfrac{\partial V}{\partial z_j}(z_2, \ldots, z_{c_n-2}, \infty)\right) = 1\right\}_{j=2,\ldots,c_n-2}$ *coincides with the hyperbolicity equations.*
If $(\zeta_2, \ldots, \zeta_{c_n-2})$ is the solution of the equations such that $\mathrm{Im}(\zeta_j) > 0$, then

$$\mathrm{Vol}(S^3 - L) = -\mathrm{Im}(V(\zeta_2, \ldots \zeta_{c_n-2}, \infty))\,.$$

Remark. These equations also coincides with the hyperbolicity equations of the canonical decomposition of $S^3 - L$. If L is a twist knot there is the solution $(\zeta_2, \ldots, \zeta_{c_n-2})$ which satisfies $\mathrm{Im}(\zeta_j) > 0$. ([15])

2.4 Example

In this section we consider the 2-bridge knot $C(3,2) = 5_2$. The labeling of the knot 5_2 is as illustrated in Figure 2.18.

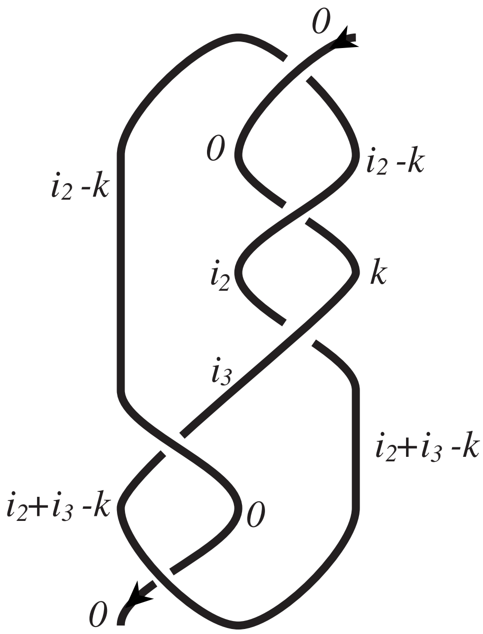

Figure 2.18: Labeling of 5_2.

Then the colored Jones polynomial of 5_2 is described as follows.

$$J_N(5_2) = \sum_{i_2,i_3,k} (-1)^{i_3} \frac{((q)_{i_2})^2 (q)_k}{((q^{-1})_{i_3})^2 (q^{-1})_{i_2-k} (q)_{k-i_3}} \, q^{-\frac{5}{4}N^2 - i_2^2 - \frac{i_3^2}{2} - i_2 i_3 - 2i_2 - i_3 + k - \frac{3}{4}}.$$

Put $q^{i_2} = z_2, q^{-i_3} = z_3, q^k = 1/w$, then the function $V(z_2, z_3, w)$ is described as follows,

$$\begin{aligned} V(z_2,z_3,w) &= -2\mathrm{Li}_2(z_2) - 2\mathrm{Li}_2(z_3) - \mathrm{Li}_2\left(\frac{1}{w}\right) - \mathrm{Li}_2\left(\frac{1}{z_2 w}\right) + \mathrm{Li}_2\left(\frac{z_3}{w}\right) \\ &\quad -(\log z_2)^2 - \frac{(\log z_3)^2}{2} + \log z_2 \log z_3 + \log(-1)\log z_3 + \frac{5}{6}\pi^2. \end{aligned}$$

Then the equations $\exp\left(z_j \dfrac{\partial V}{\partial z_j}(z_2, z_3, \infty)\right) = 1$ are as follows.

$$\left(1 - \frac{1}{z_2}\right)^2 z_3 = 1, \quad -\frac{z_2(1-z_3)^2}{z_3} = 1.$$

One of the solution of this equations is

$$z_2 = 0.539798 + 0.182582\sqrt{-1}, \quad z_3 = 0.21508 + 1.30714\sqrt{-1},$$

then $V(z_2, z_3, \infty) = 3.02413 - 2.82812\sqrt{-1}$. Actually the volume of $S^3 - 5_2$ is $2.82812\ldots$.

On the other hand, from Figure 2.12 and Figure 2.19 we can draw the triangulation of the cusp neighbourhood as illustrated in Figure 2.20.

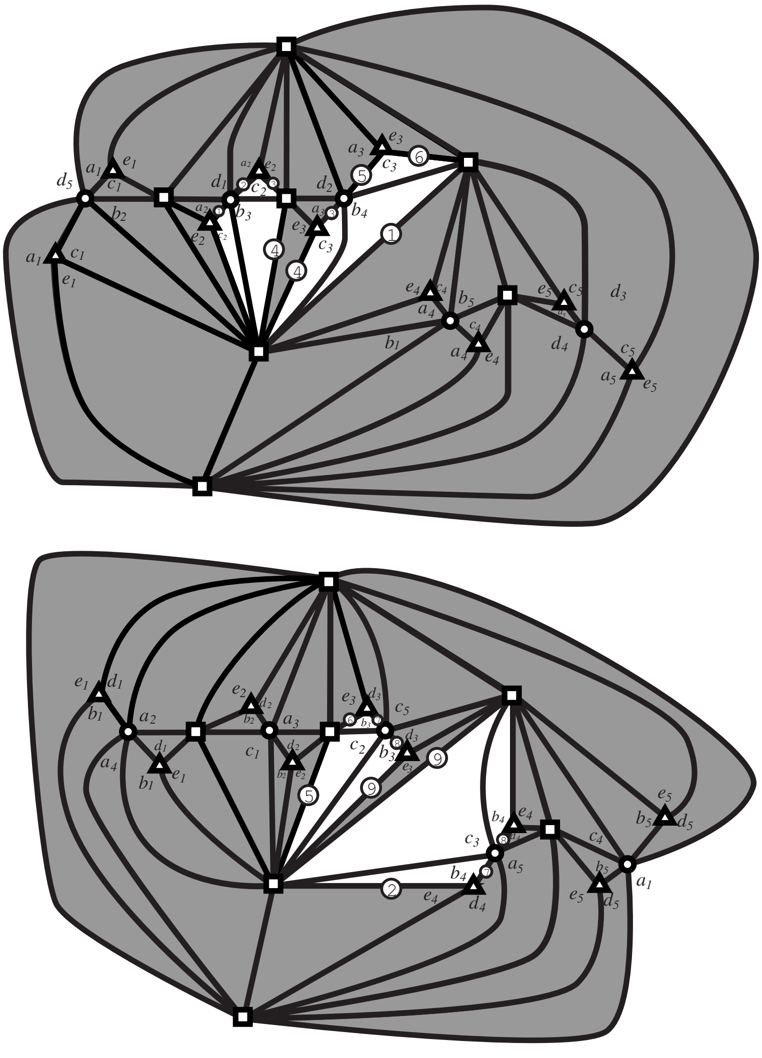

Figure 2.19: The triangulation of $\partial N(\pm)$. The edges with same numbers are identified and 12 triangles survive.

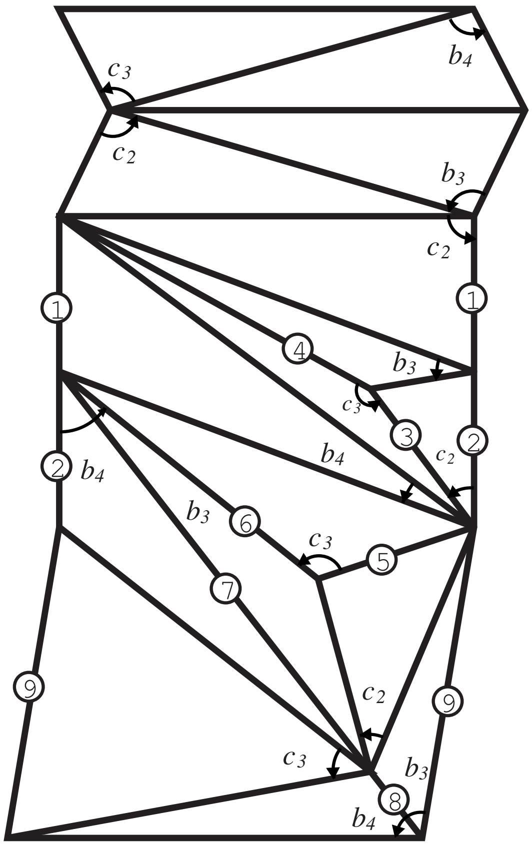

Figure 2.20: The cusp neighbourhood of $S^3 - 5_2$.

We can read the hyperbolicity equations from Figure 2.20. We put $z_2 = b_3 = c_2$ and $z_3 = b_4 = c_3$, then the hyperbolicity equations are described as follows.

$$\left(1 - \frac{1}{z_2}\right)^2 z_3 = 1, \quad -\frac{z_2(1-z_3)^2}{z_3} = 1.$$

2.5 Colored Jones polynomials of twist knots and hyperbolic structures

Let K_p be a twist knot as illustrated in Figure 2.21. In [18] we can describe the colored Jones polynomial of a twist knot K_p as follows.

$$\begin{aligned} J_N(K_p; q) &= \sum_{k=0}^{\infty} (-1)^{k+1} q^{\frac{k^2}{2} + \frac{3}{2}k} \frac{(q)_{N-1}(q)_{N+k}}{(q)_N (q)_{N-k-1}} \\ &\quad \sum_{l=0}^{k} (-1)^l q^{(l^2+l)p + \frac{l^2}{2} - \frac{l}{2}} \frac{(q)_{2l+1}}{(q)_{2l}} \frac{(q)_k}{(q)_{n+k+1}(q)_{n-k}} \end{aligned}$$

This formula is obtained by using the skein theory.

Optimistically we expect

$$2\pi \lim_{N\to\infty} \frac{\log |J_N(K_p; q)|}{N} = \mathrm{Im} H(z_0, w_0),$$

where

$$\begin{aligned} H(z,w) &= -3\mathrm{Li}_2(z) + \mathrm{Li}_2(zw) + \mathrm{Li}_2(z/w) \\ &\quad + \frac{1}{2}(\log w)^2 + p(\log w)^2 + \pi\sqrt{-1}\log w + \frac{\pi^2}{6}, \end{aligned}$$

and (z_0, w_0) is one solution of $dH/dz = 0$ and $dH/dw = 0$. This approximation is not justified as explained in Chapter 1. But we can prove the following lemma by using the decomposition of the complement of the Whitehead link discussed in [20] and [28].

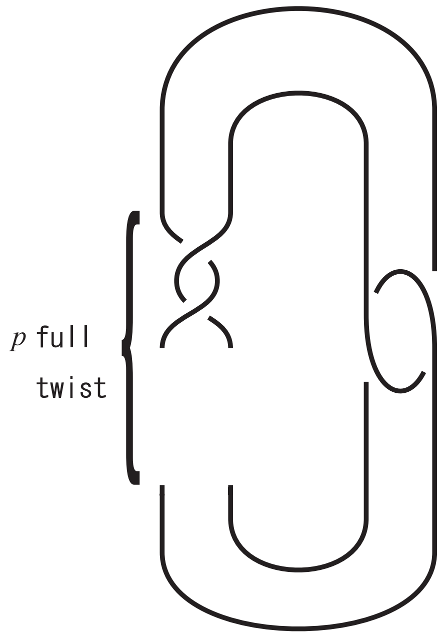

Figure 2.21: Twist knot K_p.

Lemma 2.1. *We have*

$$\mathrm{Im} H(z_0, w_0) = \mathrm{Vol}(S^3 - K_p),$$

for the suitable solution (z_0, w_0).

To prove this lemma, we review hyperbolic structures of the Whitehead link.

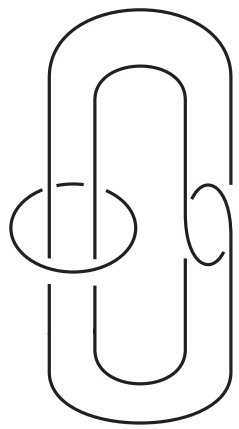

Figure 2.22: Whitehead link W

The complement of the Whitehead link W in the three-sphere S^3 is obtained from an ideal octahedron in the hyperbolic space. In [36] if we identify faces of an ideal octahedron in pairs as illustrated in Figure 2.23 then we obtain $S^3 - W$. If this ideal octahedron is the regular ideal octahedron whose all dihedral angles are $\frac{\pi}{4}$, we obtain the complete hyperbolic structure on $S^3 - W$. By deforming this octahedron we obtain incomplete hyperbolic structures on $S^3 - W$ whose metric completion are coincide with the manifold obtained from the generalized Dehn surgery along W. As in [36] we can describe Dehn surgery parameters $(p_i q_i)$ for each cusp on $S^3 - W$ by using complex parameters associated with 4 tetrahedra in an ideal octahedron as in Figure 2.24.

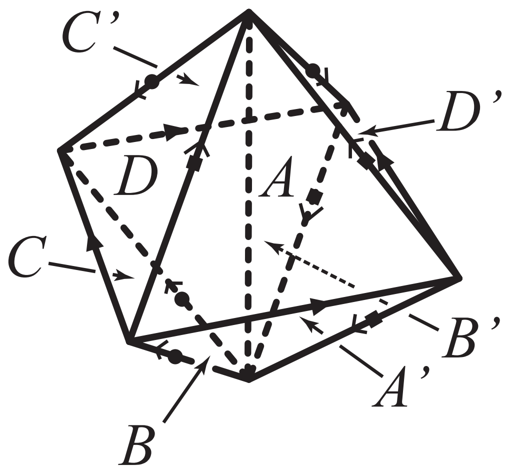

Figure 2.23: Identifying face A with A', B with B', C with C' and D with D', so as to respect the labelings of the edges.

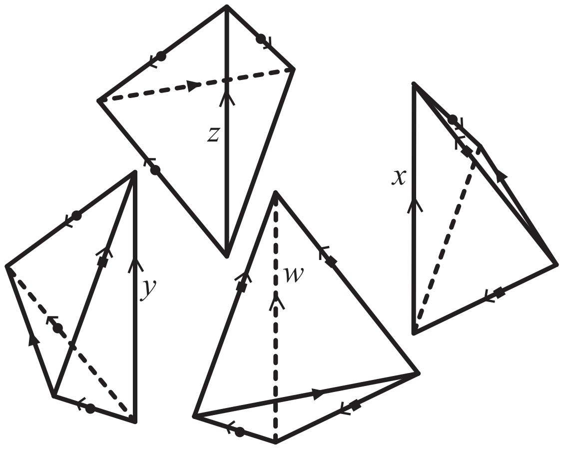

Figure 2.24: An ideal octahedron is decomposed ant 4 tetrahedra with complex parameters x, y, z and w.

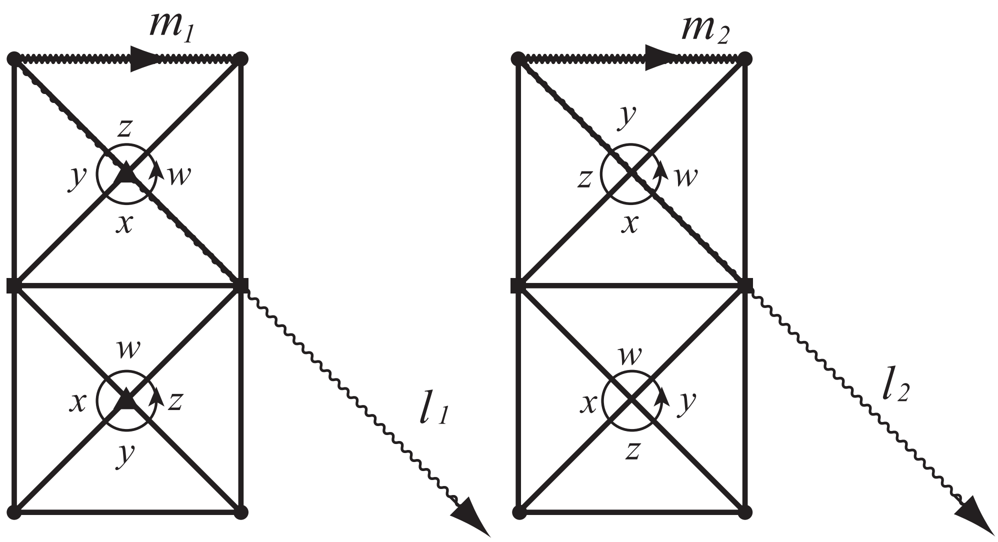

Figure 2.25: Neighbourhood of two cusps and meridians m_i and longitudes l_i.

Now, following Thurston[36] we describe hyperbolic structures on the Whitehead link complement and hyperbolic Dehn surgeries.

First, we obtain the consistency relation at four edges from Figure 2.25. So we have

$$\begin{aligned}
&xwyz = 1,\\
&\frac{1}{1-z}\left(1-\frac{1}{w}\right)\frac{1}{1-y}\left(1-\frac{1}{z}\right)\frac{1}{1-y}\left(1-\frac{1}{x}\right)\frac{1}{1-z}\left(1-\frac{1}{y}\right) = 1,\\
&\frac{1}{1-w}\left(1-\frac{1}{x}\right)\frac{1}{1-w}\left(1-\frac{1}{z}\right)\frac{1}{1-x}\left(1-\frac{1}{w}\right)\frac{1}{1-x}\left(1-\frac{1}{y}\right) = 1.
\end{aligned}$$

These relations simplify to the two relations.

$$xyzw = 1 \tag{2.12}$$

$$(1-x)(1-y)(1-z)(1-w) = 1 \tag{2.13}$$

Next, we describe the holonomy of the meridians which mean the simple closed curve that is homologous to 0 in the tubular neighbourhood of W and the longitudes which mean the simple closed curve that is homologous to 0 in $S^3 - W$. Let u_i describe the holonomy of the meridian for ith component of$W$ and v_i describe the holonomy of the longitude for ith component of$W$. From Figure 2.25 we can read u_i and v_i as follows.

$$u_1 = \log(w-1) + \log x + \log y - \log(y-1) - \pi\sqrt{-1} \tag{2.14}$$

$$v_1 = 2\log x + 2\log y - 2\pi\sqrt{-1} \tag{2.15}$$

$$u_2 = \log(w-1) + \log x + \log z - \log(z-1) - \pi\sqrt{-1} \tag{2.16}$$

$$v_2 = 2\log x + 2\log z - 2\pi\sqrt{-1} \tag{2.17}$$

The Dehn surgery parameters (p_1, q_1) and (p_2, q_2) are determine by the following equations with consistency relations.

$$p_1u_1 + q_1v_1 = 2\pi\sqrt{-1}p_2u_2 + q_2v_2 = 2\pi\sqrt{-1} \tag{2.18}$$

For the complete hyperbolic structure on S^3-W we have $u_1 = v_1 = u_2 = v_2 = 0$, which implies $x = y = z = w = \sqrt{-1}$.

We consider generalized Dehn surgeries on one cusp of $S^3 - W$. Let the first cusp be complete, so we always have $(p_1, q_1) = \infty$. This means $u_1 = v_1 = 0$. From the equation (2.15) and $v_1 = 0$ we have $x = -\frac{1}{y}$. Then the equation (2.12) deduces $z = -\frac{1}{w}$, and (2.13) gives $y = w$. So we have

$$(x, y, z, w) = \left(x, -\frac{1}{x}, x, -\frac{1}{x}\right).$$

Conversely $(x, y, z, w) = \left(x, -\frac{1}{x}, x, -\frac{1}{x}\right)$ satisfies consistency relations and $u_1 = v_1 = 0$ and thus gives a structure on $S^3 - W$ which is complete at the first cusp. So we consider only one complex parameter x with $\mathrm{Im}(x) > 0$ to describe generalized Dehn surgeries on one cusp of $S^3 - W$. The relations (2.16) and (2.17) is described as follows.

$$\begin{aligned} u_2 &= \log x + \log(x+1) - \log(x-1)\,, \\ v_2 &= 4\log x - 2\pi\sqrt{-1}\,. \end{aligned}$$

And the Dehn surgery parameter (p_2, q_2) is determined by

$$p_2 u_2 + q_2 v_2 = 2\pi\sqrt{-1}\,. \tag{2.19}$$

If the Dehn surgery parameter $(p_2, q_2) = (1, -p)$ and the parameter x satisfy (2.19) then we obtain the complete hyperbolic structure that coincides with the complete hyperbolic structure on the complement of twist knot K_p in the three-sphere. So we have the equation that describe the complete hyperbolic structure on the complement of K_p as follows.

$$(1-4p)\log x + \log(x+1) - \log(x-1) = 2(1-p)\pi\sqrt{-1}\,. \tag{2.20}$$

proof of Lemma 2.1. To find critical points of H we must solve following equations.

$$\frac{\partial H}{\partial z} = \frac{1}{z}\left(3\log(1-z) - \log(1-zw) - \log\left(1-\frac{z}{w}\right)\right) = 0\,, \tag{2.21}$$

$$\frac{\partial H}{\partial w} = \frac{1}{w}\Big(-\log(1-zw) + \log\left(1-\frac{z}{w}\right) + \log w + 2p\log w + \pi\sqrt{-1}\Big) = 0\,. \tag{2.22}$$

Here we put

$$z = 1 - \frac{1}{x} + x, \quad w = x^{-2}.$$

Then the equations (2.21) and (2.22) simplify to

$$\frac{\partial H}{\partial z} = 0 \tag{2.23}$$

$$\frac{\partial H}{\partial w} = (1-4p)\log x + \log(x+1) - \log(x-1) = 0 \tag{2.24}$$

The equation (2.24) coincide with the equation (2.20), so the solution x_0 of (2.24) describe the complete hyperbolic structure on the twist knot complement. Here as in [15] we can take x_0 such that $\mathrm{Im}(x_0) > 0$.

Next we will prove

$$\mathrm{Im}(H(z_0, w_0)) = \mathrm{Im}\left(H\left(1 - \frac{1}{x_0} + x_0, {x_0}^{-2}\right)\right) = \mathrm{Vol}(S^3 - K_p).$$

By using equations (2.21) and (2.21) we have

$$\mathrm{Im}(H(z_0, w_0)) = -3D(z_0) + D\left(\frac{z_0}{w_0}\right) + D(z_0 w_0), \tag{2.25}$$

where $D(z)$ is the Wigner-Bloch dilogarithm function defined as

$$D(z) = \operatorname{Im} \operatorname{Li}_2(z) + \log|z| \arg(1-z).$$

As in [17] the Wigner-Bloch dilogarithm function satisfies following functional equations.

$$\begin{aligned} &D(z) = -D(1-z) = -D\left(\frac{1}{z}\right), \\ &D(z^2) = 2D(z) + 2D(-z), \\ &D(z) + D(w) = D(zw) + D\left(\frac{z(1-w)}{1-zw}\right) + D\left(\frac{w(1-z)}{1-zw}\right). \end{aligned}$$

By using these formulas (2.25) simplifies to

$$-3D(z_0) + D\left(\frac{z_0}{w_0}\right) + D(z_0 w_0) = 2D(x_0) + D\left(-\frac{1}{x_0}\right) = \operatorname{Vol}(S^3 - K_p).$$

So we have proved Lemma 2.1. □

Chapter 3

Generalized Volume Conjecture

In this section, we discuss the generalization of the volume conjecture. Main result in this chapter is that the colored Jones polynomial of the Borromean rings is some cases determines the hyperbolic volume of the cone manifold with singurality along the Borromean rings.

3.1 Generalized volume conjecture

In [9] S. Gukov discussed the relation between the colored Jones polynomial evaluated at $\exp\left(a\sqrt{-1}/N\right)$ with a fixed complex number a and the A-polynomial of a knot and the volume and the Chern-Simons invariant of a three-manifold obtained from Dehn surgery along the knot.

Let $J_N(K;q)$ be the colored Jones polynomial of a knot K. In [23] it was proved that for the figure eight knot E the limit of $\frac{J_N(E;\exp(a\sqrt{-1}/N))}{N}$ for a fixed real number a near 2π determines the volume of the cone-manifold with singurality along the figure-eight knot. Moreover it was proved in [27] that the limit of $\frac{J_N(E;\exp(\alpha\sqrt{-1}/N))}{N}$ for complex number α near the unit circle determines the Neumann-Zagier function. In [24] it was proved $J_N(E;\exp(\alpha/N))$ for a complex number α with $|2\cosh\alpha-2|<1$ and $|\mathrm{Im}\alpha|<\frac{\pi}{3}$ converges and its limit is equal to the inverse of the Alexander polynomial.

In [6] it was proved that for every knot the colored Jones polynomial evaluated at $\exp(\alpha\sqrt{-1}/N)$ for a fixed small real number α grows subexponentially.

3.2 The case of the Borromean rings

In this section, we consider the colored Jones polynomial of the Borromean rings B evaluated at $\exp(2\pi r\sqrt{-1}/N)$ for a fixed real number r. Let $\Lambda(z)$ be the Lobachevsky function defined as $\Lambda(z)=-\int_0^z \log|2\sin t|dt$. We define two functions $V_1(r)$ and

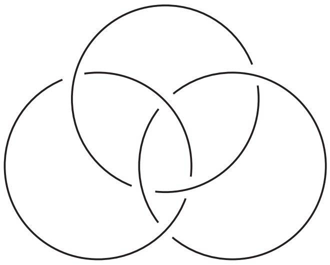

Figure 3.1: Borromean rings.

$V_2(r)$ as follows.

$$\begin{aligned} V_1(r) &= 2\left(3(\Lambda(\pi r+\theta)-\Lambda(\pi-\theta))-4\Lambda(\theta+\pi/2)-2\Lambda(\theta)\right), \\ V_2(r) &= 2\left(-3(\Lambda(\phi+\pi r)+\Lambda(\phi-\pi r))+4\Lambda(\phi+\pi/2)+2\Lambda(\phi)\right), \end{aligned}$$

where $\theta=\theta(r)$ and $\phi=\phi(r)$, $0<\theta,\phi<\frac{\pi}{2}$ are principal parameters defined by conditions

$$\begin{aligned} &T=\tan\theta,\ T^4-(3\tan^2(\pi r)+1)T^2-\tan^6(\pi r)=0, \\ &T'=\tan^2\phi, \\ &T'^3-3\tan^2(\pi r)T'^2+(\tan^6(\pi r)+6\tan^4(\pi r)+3\tan^2(\pi r)+1)T'-\tan^6(\pi r)=0. \end{aligned}$$

Let r_1 and r_2 be the solution of the equation $V_1(r)=V_2(r)$ and $0<r_1<r_2<1$ as in Figure 3.2. Then we have the following theorem.

Theorem 3.1. *Let r be the irrational number satisfying $r_2<r<1+r_1$. Then*

$$2\pi\lim_{N\to\infty}\frac{\log\left|J_N(B;\exp(2\pi r\sqrt{-1}/N))\right|}{N}=\frac{1}{r}V_1(r).$$

Here $V_1(r)$ coincides with the hyperbolic volume of the cone manifold whose underlying space is the three-sphere and whose singular set consists of three components of the Borromean rings with cone angles $2\pi|1-r|$, $2\pi|1-r|$ and $2\pi|1-r|$ [19].

3.3 The proof of Theorem 3.1

First we review how to compute colored Jones polynomials by using the Kauffman bracket skein module.

Let M be a 3-manifold. The Kauffman bracket skein module $\mathcal{S}(M)$ of M is the vector space over $\mathbb{C}[A^{\pm1}]$ spanned by isotopy classes of framed links in M and subject to the relations $-A$ $-A^{-1}$ and $+A^2+A^{-2}$, where the links in each expression are identical except in a ball in which they are depicted.

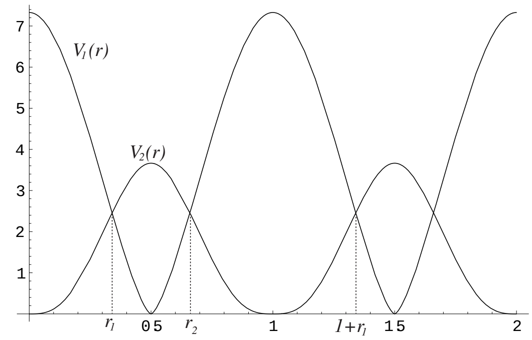

Figure 3.2: $V_1(r)$ and $V_2(r)$ for $0 < r < 2$.

The skein module of the 3-space $\mathbb{R}^3$ is the vector space over $\mathbb{C}[A^{\pm 1}]$ spanned by the empty link and identified with $\mathbb{C}[A^{\pm 1}]$. If L is a framed link in $\mathbb{R}^3$, then its value in $\mathcal{S}(\mathbb{R}^3) \cong \mathbb{C}[A^{\pm 1}]$ is the Kauffman bracket $\langle L \rangle$ of L.

The skein module of the solid torus $D^2 \times S^1$ has an algebra structure and identified with the polynomial algebra $\mathbb{C}[A^{\pm 1}][z]$ where z is identified with the circle $\{0\} \times S^1$ and the empty link is identified with 1. We take the another basis $\{e_n\}$ of this skein module instead of $\{1, z, z^2, \dots\}$ defined by $e_0 = 1$, $e_1 = z$, and $e_n = z e_{n-1} - e_{n-2}$.

For a framed link L with m components in $\mathbb{R}^3$ and α in $\mathcal{S}(D^2 \times S^1)$ we define $\langle L^\alpha \rangle$ in $\mathcal{S}(\mathbb{R}^3)$ as the link obtained from replacing each component of L with α. We define the colored Jones polynomial $J_N(L;q)$ of a link L by

$$J_N(L;q) = \frac{(-1)^{m(N-1)} \langle L^{e_{N-1}} \rangle}{[N]} \Big|_{A = -q^{1/4}},$$

where $[N] = \dfrac{A^{2N} - A^{-2N}}{A^2 - A^{-2}}$. $J_N(L;q)$ is also defined as the quantum invariant derived from the N-dimensional representation of sl_2 (see [31]).

Let $q_r = \exp(2\pi r \sqrt{-1}/N)$, r be the irrational number and B be the Borromean rings. In [14] we can describe $\langle e_{N-1}, e_{N-1}, e_{N-1} \rangle_B$ as

$$\langle e_{N-1}, e_{N-1}, e_{N-1} \rangle_B = \sum_{i=0}^{N-1} (-1)^i (A^2 - A^{-2})^{4i} \left(\frac{[N+i]!}{[N-i-1]!} \right)^3 \left(\frac{[i]!}{[2i+1]!} \right)^2 .$$

So we have $J_N(B;q_r)$ as follows.

$$\begin{aligned} & J_N(B;q_r) \\ &= (2\sin\pi r)^2 \sum_{i=0}^{N-1} \frac{\left\{\prod_{k=1}^{i} 4\sin\left(\frac{kr\pi}{N}+\pi r\right)\sin\left(\frac{kr\pi}{N}-\pi r\right)\right\}^3}{\left(\prod_{k=i+1}^{2i+1} 2\sin\left(\frac{kr\pi}{N}\right)\right)^2} \\ &= (2\sin\pi r)^2 \sum_{i=0}^{N-1} f(i). \end{aligned}$$

Note that $\sin(\pi r) \neq 0$ and $\sin\left(\frac{kr\pi}{N}\right) \neq 0$ for any $0 < k \leq 2N-1$ since r is irrational. Putting $g(i) = f(i)/f(i-1)$ then we have

$$\begin{aligned} g(i) &= \frac{\left\{4\sin\left(\frac{ir\pi}{N}+\pi r\right)\sin\left(\frac{ir\pi}{N}-\pi r\right)\right\}^3\left(2\sin\frac{ir\pi}{N}\right)^2}{\left\{4\sin\left(\frac{2ir\pi}{N}\right)\sin\left(\frac{(2i+1)r\pi}{N}\right)\right\}^2} \\ &= \frac{\left\{4\sin\left(\frac{ir\pi}{N}+\pi r\right)\sin\left(\frac{ir\pi}{N}-\pi r\right)\right\}^3\left(2\sin\frac{ir\pi}{N}\right)^2}{\left\{4\sin^2\left(\frac{2ir\pi}{N}\right)\right\}^2} + \varepsilon. \end{aligned}$$

Here ε is defined as follows.

$$\frac{\left\{4\sin\left(\frac{ir\pi}{N}+\pi r\right)\sin\left(\frac{ir\pi}{N}-\pi r\right)\right\}^3\left(2\sin\frac{ir\pi}{N}\right)^2}{\left\{4\sin^2\left(\frac{2ir\pi}{N}\right)\right\}^2}\varepsilon' = \varepsilon,$$

$$\left\{\frac{\sin\left(\frac{2ir\pi}{N}\right)}{\sin\left(\frac{(2i+1)r\pi}{N}\right)}\right\}^2 = 1+\varepsilon'.$$

For the sufficiently large N $|\varepsilon'|$ is very small, and so is $|\varepsilon|$. Therefore we can ignore ε in the limit of $J_N(B;q_r)$. Let $h(i) = g(i) - \varepsilon$. Then we rewrite $J_N(B;q_r)$ as follows.

$$J_N(B;q_r) = (2\sin\pi r)^2 \sum_{i=0}^{N-1} f(0) \prod_{k=1}^{i} h(k) + O(\varepsilon).$$

If we regard $h(i)$ as the continuous function then we have the following lemma by simple calculations.

Lemma 3.1. *If $h(i) = 1$ we have*

$$T = \tan\left(\frac{\pi r i}{N}\right), \ (T^2+1)(T^4 - (3\tan^2(\pi r)+1)T^2 - \tan^6(\pi r)) = 0.$$

If $h(i) = -1$ we have

$$T' = \tan^2\left(\frac{\pi r i}{N}\right),$$
$$T'^3 - 3\tan^2(\pi r)T'^2 + (\tan^6(\pi r) + 6\tan^4(\pi r) + 3\tan^2(\pi r) + 1)T' - \tan^6(\pi r) = 0.$$

If $h(i) = 0$ *we have*

$$i = \begin{cases} \frac{N(1-r)}{r} & \frac{1}{2} < r < 1 \\ \frac{N(2-r)}{r}, \frac{N(r-1)}{r} & 1 < r < 2 \end{cases}$$

Let $A = \frac{N\phi}{\pi r}$, $D = \frac{N(\pi-\theta)}{\pi r}$ and $[x]$ denote the greatest integer that is less than or equal to x. Then we have the following lemma.

Lemma 3.2.

$$\begin{aligned} 2\pi r \lim_{N\to\infty} \frac{\log|f([A])|}{N} &= V_2(r), \\ 2\pi r \lim_{N\to\infty} \frac{\log|f([D])|}{N} &= V_1(r). \end{aligned}$$

Proof. We will show the second formula. We have

$$\begin{aligned} &\lim_{N\to\infty} \frac{\log|f([D])|}{N} \\ &= 3 \lim_{N\to\infty} \frac{1}{N} \sum_{k=0}^{[D]} \left(\log\left|2\sin\left(\frac{kr\pi}{N} + \pi r\right)\right| + \log\left|2\sin\left(\frac{kr\pi}{N} - \pi r\right)\right| \right) \\ &\quad -2 \lim_{N\to\infty} \frac{1}{N} \sum_{k=[D]+1}^{2[D]+1} \log\left|2\sin\left(\frac{kr\pi}{N}\right)\right| \\ &= \frac{3}{\pi r}\int_{\pi r}^{\pi-\theta+\pi r} \log|2\sin z|dz + \frac{3}{\pi r}\int_{-\pi r}^{\pi-\theta-\pi r} \log|2\sin z|dz - \frac{2}{\pi r}\int_{\pi-\theta}^{2\pi-2\theta} \log|2\sin z|dz \\ &= \frac{1}{2\pi r} V_1(r). \end{aligned}$$

Here we use the formulas $\Lambda(z) = -\Lambda(-z) = \Lambda(z+\pi)$ and $\Lambda(2z) = 2\Lambda(z) + 2\Lambda\left(z+\frac{\pi}{2}\right)$. □

Let r_1 and r_2 be solutions of $V_1(r) = V_2(r)$ and $0 < r_1 < r_2 < 1$. Numerical calculations follow $r_1 = 0.340186\ldots$ and $r_2 = 0.659814\ldots$. If $r_2 < r < 1 + r_1$ then we have $V_1(r) > V_2(r)$.

First we consider the case when $r_2 < r < 1$. We put

$$A = \frac{N\phi}{\pi r}, \quad B = \frac{N(1-r)}{r}, \quad C = \frac{N\theta}{\pi r}, \quad D = \frac{N(\pi-\theta)}{\pi r}.$$

From Lemma 2.1 we note that $\sum f(i)$ is alternate sum for $i < [B]$ since $g(i) < 0$ and $f([A])$ and $f([D])$ are the local maxima. So we have

$$\left|\frac{J_N(B;q_r)}{4\sin^2(\pi r)}\right| \le \sum_{i=0}^{N-1} |f(i)| < N|f([D])|.$$

Lemma 2.2 follows

$$\frac{1}{N}\log\left|\frac{f(A)}{f(D)}\right| = \delta(N) < 0,$$
$$|f(D)| = \exp(-N\delta(N))|f(A)| > N|f(A)|$$

for the sufficiently large N. So we have the following inequality.

$$\begin{aligned}\left|\frac{J_N(B;q_r)}{4\sin^2(\pi r)}\right| &> \left|f([D]) + \sum_{i=0}^{[B]-1} f(i)\right| \\ &> |f([D]) \pm Nf([A])| = |f([D])|\left|1 \pm N\frac{f([A])}{f([D])}\right|,\end{aligned}$$

where the sign $\pm$ means the sign of $-f(D)$.

Summarizing above inequalities we have

$$|f([D])|\left|1 \pm N\frac{f([A])}{f([D])}\right| < \left|\frac{J_N(B;q_r)}{4\sin^2(\pi r)}\right| < N|f([D])|.$$

This inequalities follows

$$\lim_{N\to\infty}\frac{\log|J_N(B;q_r)|}{N} = \lim_{N\to\infty}\frac{\log|f(D)|}{N} = \frac{1}{2\pi r}V_1(r).$$

So we have proved Theorem 2 in the case when $r_2 < r < 1$.

Next we consider the case when $1 < r < 1 + r_1$. We put

$$B' = \frac{N(r-1)}{r}, \quad E = \frac{N(2-r)}{r}, \quad F = \frac{N(\pi - \phi)}{\pi r}.$$

In this case $f(i)$ take local maxima at $i = [A]$, $[D]$ and $[F]$. As Lemma 2.2 we have

$$2\pi r \lim_{N\to\infty}\frac{\log|f(F)|}{N} < 0.$$

Therefore similar arguments for the case $r_2 < r < 1$ follows the proof of Theorem 2.

3.4 Observations

Actually Theorem 2 may be extended to the case when $r > \frac{1}{2}$. We can confirm it by numerical computations as in Figure 3.3.

Intuitively the alternate sum $\displaystyle\sum_{i=1}^{[B]-1} f(i)$ may not contribute the limit and the contribution of the limit may come from $f([D])$.

We can also do similar numerical computation in the case of the Whitehead link W as in Figure 3.4.

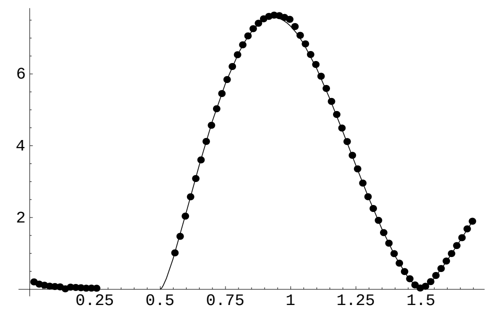

Figure 3.3: Dots indicate $2\pi\dfrac{\log|J_N(B;q_r)|}{N}$ for $N=500$ and $0<r<1.7$. The solid curve indicates the hyperbolic volume of the cone-manifold whose cone angles are all $2\pi|1-r|$.

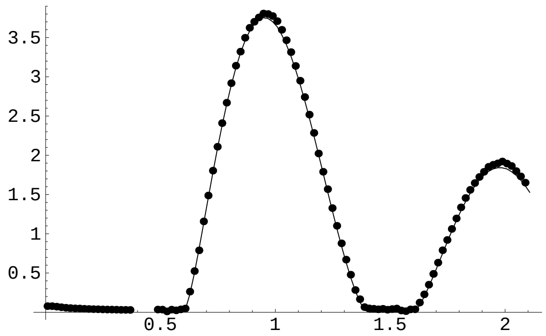

Figure 3.4: Dots indicate $2\pi\dfrac{\log|J_N(W;q_r)|}{N}$ for $N=500$ and $0<r<2.2$. The solid curve indicates the hyperbolic volume of the cone-manifold whose two cone angles are all $2\pi|1-r|$.

This example also seems to imply the relation between the colored Jones polynomial and the volume function of the hyperbolic cone-manifold.

Next, we put

$$J_N^{a,b}(B;q) := \frac{\langle e_{N-1}, e_{aN-1}, e_{bN-1}\rangle_B}{[N]}$$

We consider the limit of

$$\frac{\log\left|J_N^{a,b}(B;q_r)\right|}{N}$$

for integers a and b. We compare this limit with the following function

$$\begin{aligned} V_{a,b}(r) &= 2((\Lambda(\pi r+\theta)-\Lambda(\pi r-\theta))+(\Lambda(a\pi r+\theta)-\Lambda(a\pi r-\theta)) \\ &\quad +(\Lambda(b\pi r+\theta)-\Lambda(b\pi r-\theta))-4\Lambda(\pi/2+\theta)-2\Lambda(\theta)) \end{aligned}$$

where $\theta = \theta(r, a, b)$ is the principal parameter defined by conditions

$$T = \tan\theta,$$
$$T^4 - T^2(1 + \tan^2(\pi r) + \tan^2(a\pi r) + \tan^2(b\pi r)) - \tan^2(\pi r)\tan^2(a\pi r)\tan^2(b\pi r) = 0.$$

$V_{a,b}(r)$ coincides with the volume of the cone manifold whose underlying space is the three-sphere and whose singular set consists of three components the Borromean rings with cone angles $2\pi|1-r|$, $2\pi|1-ar|$ and $2\pi|1-br|$. We can numerically confirm that these are related to each other as in following results.

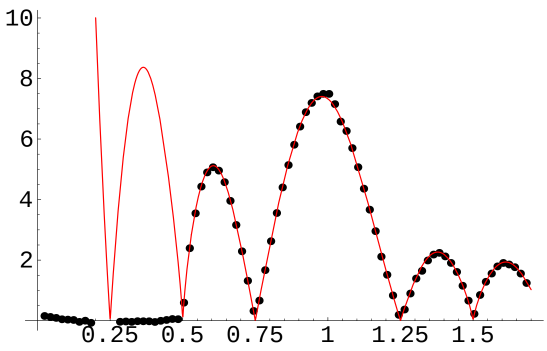

Figure 3.5: Dots indicate $2\pi \dfrac{\log \left| J_N^{2,2}(B; q_r) \right|}{N}$ for $N = 300$ and the solid curve indicates $V_{2,2}(r)/r$.

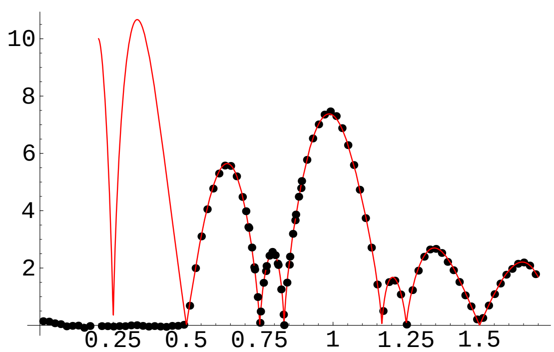

Figure 3.6: Dots indicate $2\pi \dfrac{\log \left| J_N^{2,3}(B; q_r) \right|}{N}$ for $N = 300$ and the solid curve indicates $V_{2,3}(r)/r$.

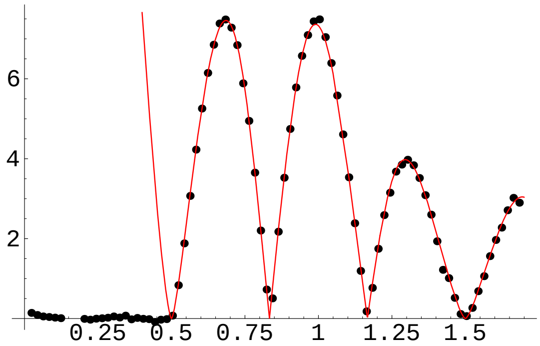

Figure 3.7: Dots indicate $2\pi \dfrac{\log \left| J_N^{3,3}(B; q_r) \right|}{N}$ for $N = 300$ and the solid curve indicates $V_{3,3}(r)/r$.

Appendix A

Optimistic limit of the Witten-Reshetikhin-Turaev invariants

In this chapter, we compute the optimistic limit of Witten-Reshetikhin-Turaev invariants of the manifolds obtained from 5_2, 6_1, and 6_3 by integral Dehn surgeries.

Let $M_p(K)$ be the closed 3-manifold obtained from S^3 by Dehn surgery along knot K with framing $p \in \mathbb{Z}$, and denote by $\tau_N(M)$ the Witten-Reshetikhin-Turaev invariant of 3-manifold M associated with the Lie group $sl_2(\mathbb{C})$ and with level $N-2$. From [13] we have the Witten-Reshetikhin-Turaev invariant of three manifold obtained from knot by integral Dehn surgery as follows.

$$\tau_N(M_p(K)) = \sqrt{\frac{2}{N}} \sin\frac{\pi}{N} \exp\left(\frac{-3\pi\sqrt{-1}}{4}\right) q^{\frac{3-p}{4}} \sum_{n=1}^{N-1} [n]^2 q^{\frac{p}{4}n^2} J_n(K;q) \ .$$

Here $q = \exp\left(\dfrac{2\pi\sqrt{-1}}{N}\right)$.

Following [22], we define the optimistic limit of WRT invariants as follows. First, we deform The WRT invariant $\tau_N(M_p(K))$ as follows.

$$\tau_N(M_p(K)) = P(N) \sum_{n_1,n_2,\ldots,n_k} q^{Q+L} \prod_a ((q)_{l_a})^{\varepsilon_a} \ ,$$

where $P(N)$ is the function of N with polynomial growth, L is linear function of $n_1, n_2, \ldots, n_k$, ε_a is equal to 1 or -1, l_a is linear function $\sum l_{ai} n_i + c$ and Q is quadratic form $\displaystyle\sum_{1\le i\le j} r_{ij} n_i n_j$. Next we formally define the function $\tilde{V}$ as follows.

$$\tilde{V}(z_1, \ldots, z_k) \quad = \quad -\sum_a \varepsilon_a \left(\mathrm{Li}_2\left(\prod_i z_i^{l_{ai}}\right) - \frac{\pi^2}{6}\right) + \sum_{i\le j} r_{ij} \log z_i \log z_j \ \cdots (*)$$

Here z_i in $\tilde{V}$ is corresponding to q^i in $\tau_N(M_p(K))$. Let $(\zeta_1,\dots,\zeta_k)$ be the critical point of $\tilde{V}$, and we define V as follows.

$$V(z_1,\dots,z_k)=\tilde{V}(z_1,\dots,z_k)+2\pi\sqrt{-1}\sum_{i=1}^{k}c_i\log z_i\ .$$

Here c_i is chosen so that $\frac{\partial\tilde{V}}{\partial z_i}(\zeta_1,\dots,\zeta_k)+2\pi\sqrt{-1}\frac{c_i}{\zeta_i}=0$ for $i=1,\dots,k$. We define the optimistic limit of $\dfrac{\log\tau_N(M_p(K))}{N}$, denoted by $\underset{N\to\infty}{\text{o-lim}}\dfrac{2\pi\sqrt{-1}\log\tau_N(M_p(K))}{N}$, as $V(\zeta_1,\dots,\zeta_k)$, where $(\zeta_1,\dots,\zeta_k)$ is some critical point of $\tilde{V}$, and o-lim is called *optimistic limit* ([22]). Since there are many critical points of V, this definition of o-lim is not well-defined. But several calculations indicate that $V(\zeta_1,\dots\zeta_k)$ for some solution is related to the volume and Chern-Simons invariant of 3-manifold.

A.1 The case of 5_2

We can describe the colored Jones polynomial of 5_2 as follows.

$$\begin{aligned}J_n(5_2,s)\ &=\ \sum_{i,j,k}\frac{(q)_i(q)_{n-1-j}(q)_{n-1}}{(q)_j(q)_{i-k}(q)_{k-j}(q)_{n-1-k}(q)_{n-1-i}}\\&\qquad q^{-\frac{5}{4}n^2+2n(i+j-k+1)-ij-ik+k^2-i-j+k-\frac{3}{4}}\end{aligned}$$

So WRT invariant of $M_p(5_2)$ is

$$\begin{aligned}\tau_N(M_p(5_2))\ &=\ \sqrt{\frac{2}{N}}\sin\frac{\pi}{N}\exp\left(\frac{-3\pi\sqrt{-1}}{4}\right)q^{\frac{3-p}{4}}\left(\frac{1}{q^{\frac{1}{2}}-q^{\frac{1}{2}}}\right)^2\\&\quad\sum_{n=1}^{N-1}\sum_{i\le j\le k}\left(\frac{(q)_n}{(q)_{n-1}}\right)^2\frac{(q)_i(q)_{n-1-j}(q)_{n-1}}{(q)_j(q)_{i-k}(q)_{k-j}(q)_{n-1-k}(q)_{n-1-i}}\\&\quad q^{\frac{p-5}{4}n^2+2n(i+j-k+1)-ij-ik+k^2-i-j+k-\frac{3}{4}}\end{aligned}$$

We define $\tilde{V_p}$ as follows.

$$\begin{aligned}\tilde{V_p}(x,y,z,w)\ &=\ -\mathrm{Li}_2(y)-\mathrm{Li}_2(x/z)-\mathrm{Li}_2(x)+\mathrm{Li}_2(z)+\mathrm{Li}_2(y/w)+\mathrm{Li}_2(w/z)\\&\quad+\mathrm{Li}_2(x/w)+\mathrm{Li}_2(x/y)+2\log x\,(\log y+\log z-\log w)\\&\quad-\log y\,(\log z+\log w)+\frac{p-5}{4}(\log x)^2+(\log w)^2-\frac{\pi^2}{3}\end{aligned}$$

From this we have algebraic equations as follows.

$$\begin{cases} \dfrac{x^{\frac{p-5}{2}}(1-x)y^3(x-z)z}{w(w-x)(x-y)} = 1 \\ \dfrac{x^2(x-y)(y-1)}{(w-y)yz} = 1 \\ \dfrac{x^2(z-w)}{y(x-z)(z-1)} = 1 \\ \dfrac{(w-x)(w-y)z}{x^2y(z-w)} = 1 \end{cases} \tag{A.1}$$

Using Mathematica 4.1, for every $p = 0, 1, \dots$ we can calculate the solutions of (A.1), and SnapPea [38] tells us the volume and Chern-Simons invariant of $M_p(5_2)$.

For example, when $p = 7$, one solution of (A.1) is

$$\begin{aligned} x_0 &= 0.253875\cdots - 0.486542\cdots\sqrt{-1}, \\ y_0 &= 0.073554\cdots - 0.321118\cdots\sqrt{-1}, \\ z_0 &= 0.686016\cdots + 0.605742\cdots\sqrt{-1}, \\ w_0 &= 0.165863\cdots - 0.099916\cdots\sqrt{-1} \end{aligned}$$

and,

$$\begin{aligned} V_7(x_0, y_0, z_0, w_0) &= \tilde{V}_7(x_0, y_0, z_0, w_0) \\ &\quad +2\pi\sqrt{-1}\,(c_1\log x_0 + c_2\log y_0 + c_3\log z_0 + c_4\log w_0) \\ &= 4.63884\cdots + 1.84359\cdots\sqrt{-1}\,. \end{aligned}$$

On the other hand, the volume of $M_7(5_2)$ is 1.8435859723, and the Chern-Simons invariant $\mathrm{cs}(M_7(5_2))$ is 0.23500640868 by using SnapPea. So we have

$$V_7(x_0, y_0, z_0, w_0) = \mathrm{CS}(M_7(5_2)) + \mathrm{Vol}(M_7(5_2))\sqrt{-1}$$

up to some digits. (Here CS:$= 2\pi^2$cs).
In a similar way we can calculate V and volumes and Chern-Simons invariants for some p as in Table A.1.

p	V_p	**Volume**	**CS**
-99	$2.926983372 + 2.8252710308\sqrt{-1}$	2.825271031	2.926983372
⋮	⋮	⋮	⋮
-30	$2.72301119 + 2.8005414863\sqrt{-1}$	2.800541486	2.72301119
-29	$2.71361574 + 2.7987788531\sqrt{-1}$	2.798778853	2.71361574
-28	$2.70362058 + 2.79684217431\sqrt{-1}$	2.7968421743	2.70362058
-27	$2.69296696 + 2.79470782272\sqrt{-1}$	2.7947078227	2.69296696
-26	$2.681588310 + 2.7923480319\sqrt{-1}$	2.792348032	2.681588310
-25	$2.669408880 + 2.78972999726\sqrt{-1}$	2.7897299973	2.669408880
-24	$2.656342124 + 2.786814740\sqrt{-1}$	2.78681474	2.656342124
-23	$2.64228873742 + 2.78355566477\sqrt{-1}$	2.7835556648	2.64228873742
-22	$2.627134261 + 2.77989670138\sqrt{-1}$	2.7798967014	2.627134261
-21	$2.610746124 + 2.7757699078\sqrt{-1}$	2.775769908	2.610746124
-20	$2.592969998 + 2.77109232763\sqrt{-1}$	2.7710923276	2.592969998
-19	$2.57362524 + 2.76576183868\sqrt{-1}$	2.7657618387	2.57362524
-18	$2.5524992123 + 2.75965160191\sqrt{-1}$	2.7596516019	2.5524992123
-17	$2.529340054 + 2.7526025447\sqrt{-1}$	2.752602545	2.529340054
-16	$2.503847583 + 2.7444130439\sqrt{-1}$	2.744413044	2.503847583
-15	$2.475661618 + 2.7348245520\sqrt{-1}$	2.734824552	2.475661618
-14	$2.4443470176 + 2.72350123965\sqrt{-1}$	2.7235012397	2.4443470176
-13	$2.40937443 + 2.7100006357\sqrt{-1}$	2.710000636	2.40937443
-12	$2.370095586 + 2.6937304242\sqrt{-1}$	2.693730424	2.370095586
-11	$2.325711866 + 2.6738834223\sqrt{-1}$	2.673883422	2.325711866
-10	$2.275235433 + 2.6493372408\sqrt{-1}$	2.649337241	2.275235433
-9	$2.217444394 + 2.61849503065\sqrt{-1}$	2.6184950307	2.217444394
-8	$2.150840861 + 2.5790247944\sqrt{-1}$	2.579024794	2.150840861
-7	$2.073643785 + 2.52741847731\sqrt{-1}$	2.5274184773	2.073643785
-6	$1.983920660 + 2.45822407834\sqrt{-1}$	2.4582240783	1.983920660
-5	$1.880198644 + 2.36270079255\sqrt{-1}$	2.3627007926	1.880198644
-4	$1.763674526 + 2.22671790391\sqrt{-1}$	2.2267179039	1.763674526
-3	$1.6449340668482 + 2.0298832128\sqrt{-1}$	2.029883213	$2\pi^2\, 1/12$
-2	$1.552551186 + 1.7571260291\sqrt{-1}$	1.757126029	1.552551186
-1	$1.512064188 + 1.41406104416\sqrt{-1}$	1.4140610442	1.512064188
0	$1.52067272 + 0.981368828892\sqrt{-1}$	0.98136882889	1.52067272
2	2.63189450695716	0	$2\pi^2 2/15$
3	3.1723728432072	0	$2\pi^2\, 9/56$

Table A.1: The calculation for $M_p(5_2)$.

4	3.73848651556	0	$2\pi^2 25/132$
6	$4.867832052 + 1.3985088841\sqrt{-1}$	1.398508884	4.867832052
7	$4.638840570 + 1.84358597232\sqrt{-1}$	1.8435859723	4.638840570
8	$4.451323510 + 2.1030952907\sqrt{-1}$	2.103095291	4.451323510
9	$4.297182738 + 2.27263186358\sqrt{-1}$	2.2726318636	4.297182738
10	$4.169388864 + 2.39011907536\sqrt{-1}$	2.3901190754	4.169388864
11	$4.06245196 + 2.4748136131\sqrt{-1}$	2.474813613	4.06245196
12	$3.972130075 + 2.5377252563\sqrt{-1}$	2.537725256	3.972130075
13	$3.895144337 + 2.58560868494\sqrt{-1}$	2.5856086849	3.895144337
14	$3.828951552 + 2.62281140368\sqrt{-1}$	2.6228114037	3.828951552
15	$3.77156882 + 2.6522338865\sqrt{-1}$	2.652233887	3.77156882
16	$3.72144006 + 2.67586788142\sqrt{-1}$	2.6758678814	3.72144006
17	$3.677335141 + 2.69511479677\sqrt{-1}$	2.651147968	3.677335141
18	$3.6382738818 + 2.71098172755\sqrt{-1}$	2.7109817276	3.6382738818
19	$3.603468965 + 2.72420606153\sqrt{-1}$	2.7242060615	3.603468965
20	$3.572282827 + 2.73533682659\sqrt{-1}$	2.7353368266	3.572282827
21	$3.544195053 + 2.74478903411\sqrt{-1}$	2.7447890341	3.544195053
22	$3.51877757 + 2.752880730\sqrt{-1}$	2.75288073	3.51877757
23	$3.495675663 + 2.75985872374\sqrt{-1}$	2.7598587237	3.495675663
24	$3.474593308 + 2.76591675307\sqrt{-1}$	2.7659167531	3.474593308
25	$3.455281826 + 2.7712085082\sqrt{-1}$	2.771208508	3.455281826
26	$3.437530974 + 2.77585709950\sqrt{-1}$	2.7758570995	3.437530974
27	$3.421161945 + 2.77996203026\sqrt{-1}$	2.7799620303	3.421161945
28	$3.406021806 + 2.78360439480\sqrt{-1}$	2.7836043948	3.406021806
29	$3.39197905 + 2.7868507959\sqrt{-1}$	2.786850796	3.39197905
30	$3.378920067 + 2.78975632836\sqrt{-1}$	2.7897563284	3.378920067
31	$3.366746164 + 2.7923668734\sqrt{-1}$	2.792366873	3.366746164
32	$3.355371297 + 2.79472087943\sqrt{-1}$	2.7947208794	3.355371297
33	$3.344720100 + 2.79685075469\sqrt{-1}$	2.7968507547	3.344720100
34	$3.334726298 + 2.79878396717\sqrt{-1}$	2.7987839672	3.334726298
35	$3.325331394 + 2.80054391778\sqrt{-1}$	2.8005439178	3.325331394
⋮	⋮	⋮	⋮
99	$3.126316390 + 2.82496716048\sqrt{-1}$	2.8249671605	3.126316390

Table A.1 (continued)

We note that for $p = 1, 5$ SnapPea can not calculate the volume of $M_p(5_2)$. In this case we can calculate V_p, but I don't know what the optimistic limit means. Also we note that when $p = \infty$, $M_\infty(5_2)$ is the complement of 5_2 in S^3. Then the suitable saddle point of $\tilde{V}_p(1, y, z, w)$ is,

$$y_0 = 0.539798 - 0.182582\sqrt{-1},\ z_0 = 0.122561 + 0.744862\sqrt{-1},\ w_0 = 0.$$

Then V_∞ is $3.02413\cdots + 2.82812\cdots\sqrt{-1}$. Using SnapPea we can see that this real part is numerically equal to $-\mathrm{CS}(M_\infty(5_2))$ and imaginary part is numerically equal to the Volume of $M_\infty(5_2)$.

A.2 The case of 6_1

We describe the colored Jones polynomial of 6_1 as follows.

$$J_n(6_1,s) = \sum_{i,j,k,l} \frac{(s)_{i+j}(s)_{j+k}(s)_{n-1}(s)_{n-1-l}(s)_{n-1-l+j}}{(s)_j(s)_{i+j-l}(s)_{j+k-l}(s)_l(s)_{l-j}(s)_{n-1-i-j}(s)_{n-1-k}(s)_{n-1-j-k}} (-1)^j q^{-\frac{1}{2}n^2-in+n+\frac{1}{2}j(3+2i-2l-2n)-l(2+i+k-2n)+\frac{3}{2}j^2-\frac{1}{2}}$$

So we have the WRT invariant of $M_p(6_1)$ as follows.

$$\begin{aligned}\tau_N(M_p(6_1)) &= \sqrt{\frac{2}{N}}\sin\frac{\pi}{N}\exp\left(\frac{-3\pi\sqrt{-1}}{4}\right) q^{\frac{3-p}{4}} \left(\frac{1}{q^{\frac{1}{2}}-q^{\frac{1}{2}}}\right)^2 \\ &\quad \sum_{n=1}^{N-1}\sum_{i,j,k,l} \frac{(q)_{i+j}(q)_{j+k}(q)_{n-1}(q)_{n-1-l}(q)_{n-1-l+j}}{(q)_j(q)_{i+j-l}(q)_{j+k-l}(q)_l(q)_{l-j}(q)_{n-1-i-j}(q)_{n-1-k}(q)_{n-1-j-k}} \\ &\quad \left(\frac{(q)_n}{(q)_{n-1}}\right)^2 (-1)^j q^{\frac{p-2}{4}n^2-in+n+\frac{1}{2}j(3+2i-2l-2n)-l(2+i+k-2n)+\frac{3}{2}j^2-\frac{1}{2}}\end{aligned}$$

Assigning x, y, z, w, and$u$ with q^n, q^i, q^j, q^k, and q^l, we define $\tilde{V}_p$ as follows.

$$\begin{aligned}\tilde{V}_p(x,y,z,w,u) &= -\mathrm{Li}_2(yz)-\mathrm{Li}_2(zw)-\mathrm{Li}_2(x)-\mathrm{Li}_2(x/u)-\mathrm{Li}_2(xz/u)+\mathrm{Li}_2(z) \\ &\quad +\mathrm{Li}_2(yz/u)+\mathrm{Li}_2(zw/u)+\mathrm{Li}_2(u)+\mathrm{Li}_2(u/z)+\mathrm{Li}_2(x/(yz)) \\ &\quad +\mathrm{Li}_2(x/w)+\mathrm{Li}_2(x/(zw))+\frac{p-2}{4}(\log x)^2+\frac{3}{2}(\log z)^2 \\ &\quad -\log x(\log y+\log z-2\log u)+\log y(\log z-\log u) \\ &\quad -\log z\log u-\log w\log u+\log(-1)\log z-\frac{\pi^2}{2}\end{aligned}$$

So we describe algebraic equations as follows.

$$\begin{cases} \dfrac{w^2(u-x)(x-1)x^{1-\frac{p}{2}}z(u-xz)}{(x-w)(x-wz)(x-yz)} = 1 \\ \dfrac{(x-yz)(yz-1)}{xy(u-yz)} = 1 \\ \dfrac{(z-u)(x-wz)(wz-1)(u-xz)(x-yz)(yz-1)}{wx(z-1)(u-wz)(u-yz)} = 1 \\ \dfrac{(w-x)(wz-1)(wz-x)}{(wz-u)w^2z} = 1 \\ \dfrac{x^2(u-wz)(u-yz)}{(u-1)w(u-x)y(u-z)(u-xz)} = 1 \end{cases} \tag{A.2}$$

For some p we have the solution of (A.2) and V_p up to some digits as in Table A.2 (p.62).

p	V_p	**Volume**	π^2−CS
-10	$7.70347582 + 2.93636141399\sqrt{-1}$	2.936361414	7.70347582
-9	$7.789780077 + 2.88839206790\sqrt{-1}$	2.8883920679	7.789780077
-8	$7.892362946 + 2.8241218340\sqrt{-1}$	2.824121834	7.892362946
-7	$8.015561282 + 2.73559311366\sqrt{-1}$	2.7355931137	8.015561282
-6	$8.164954530 + 2.60954395516\sqrt{-1}$	2.6095439552	8.164954530
-5	$8.347510420 + 2.42246251687\sqrt{-1}$	2.4224625169	8.347510420
-4	$8.571369022 + 2.1280124612\sqrt{-1}$	2.128012461	8.571369022
-3	$8.843514347 + 1.6104697112\sqrt{-1}$	1.610469711	8.843514347
0	6.853891945	0	$\pi^2 - 2\pi^2\, 11/72$
1	6.200136098	0	$\pi^2 - 2\pi^2\, 29/156$
3	$4.867832052 + 1.39850888415\sqrt{-1}$	1.3985088842	$\pi^2 - (-4.86783)$
4	$5.016625226 + 1.9415030840\sqrt{-1}$	1.941503084	5.016625226
5	$5.19081723 + 2.29443830007\sqrt{-1}$	2.2944383001	5.19081723
6	$5.3635119190 + 2.5274184773\sqrt{-1}$	2.527418477	5.3635119190
7	$5.516829612 + 2.68222673214\sqrt{-1}$	2.6822267321	5.516829612
8	$5.646891453 + 2.78812981321\sqrt{-1}$	2.7881298132	5.646891453
9	$5.756041991 + 2.86315445462\sqrt{-1}$	2.8631544546	5.756041991
10	$5.847897738 + 2.9180399572\sqrt{-1}$	2.918039957	5.847897738
11	$5.925781540 + 2.9593195859\sqrt{-1}$	2.959319586	5.925781540
12	$5.9924065954 + 2.9911069054\sqrt{-1}$	2.991106905	5.9924065954
13	$6.049910780 + 3.0160830308\sqrt{-1}$	3.016083031	6.049910780
14	$6.099964613 + 3.03605117229\sqrt{-1}$	3.0360511723	6.099964613
15	$6.143876469 + 3.0522582285\sqrt{-1}$	3.052258229	6.143876469
16	$6.182678054 + 3.0655877261\sqrt{-1}$	3.065587726	6.182678054
17	$6.217189919 + 3.07667933643\sqrt{-1}$	3.0766793364	6.217189919
18	$6.248070665 + 3.0860050982\sqrt{-1}$	3.086005098	6.248070665
19	$6.275853746 + 3.09391931789\sqrt{-1}$	3.0939193179	6.275853746
20	$6.3009750785 + 3.10069201347\sqrt{-1}$	3.1006920135	6.3009750785
21	$6.32379387 + 3.10653180841\sqrt{-1}$	3.10635318084	6.32379387
22	$6.344608475 + 3.1116019044\sqrt{-1}$	3.111601904	6.344608475

Table A.2: The calculation for $M_p(6_1)$.

23	$6.363668540 + 3.116031420\sqrt{-1}$	3.11603142	6.363668540
24	$6.381184417 + 3.1199235680\sqrt{-1}$	3.119923568	6.381184417
25	$6.397334504 + 3.1233616341\sqrt{-1}$	3.123361634	6.397334504

Table A.2 (continued)

We note that for p=2 SnapPea cannot tell us the volume of $M_p(6_1)$. When $p = -1, -2$ $M_p(6_1)$ is Seifert fibered manifold and it's volume is 0, and I did not find the suitable solution of (A.2) and I don't know what the real part of V_p means. Also we note that when $M_p(6_1)$ is the complement of 6_1 in S^3 (that is $p = \infty$), we can calculate the stationary point for $\tilde{V}_\infty(1, x, y, z, w)$, and we get

$$V_\infty = -6.7907415\cdots + 3.1639632\cdots\sqrt{-1}$$

By using SnapPea, the next equation holds up to some digits.

$$V_\infty = \mathrm{CS}(M_\infty(6_1)) + \mathrm{Vol}(M_\infty(6_1))\sqrt{-1} \qquad (\mathrm{mod}\ \pi^2)$$

A.3 The case of 6_3

From [26], the colored Jones polynomial of 6_3 is as follows.

$$J_n(6_3; s) = \sum_{k,l,m} \frac{(s)_{k+l+m}(s)_{n-1}(s)_{n+m}(s)_{n-1-k}(s)_{n-1-l}}{(s)_k(q)_l(s)_m(s)_n(s)_{n-1-k-m}(s)_{n-1-l-m}(s)_{n-1-k-l-m}} (-1)^{k+m} s^{\frac{1}{2}(m^2+m+k^2-k+2l+2lm-4mn-2kn)}$$

We define $\tilde{V}_p$ as follows.

$$\begin{aligned}\tilde{V}_p(x, y, z, w) = & -\mathrm{Li}_2(xw) - \mathrm{Li}_2(x/y) - \mathrm{Li}_2(x/z) - \mathrm{Li}_2(yzw) + \mathrm{Li}_2(y) \\ & +\mathrm{Li}_2(z) + \mathrm{Li}_2(w) + \mathrm{Li}_2(x/(yw)) + \mathrm{Li}_2(x/(zw)) \\ & +\mathrm{Li}_2(x/(yzw)) + \log(-1)(\log y + \log w) + \frac{1}{2}(\log w)^2 \\ & +\frac{1}{2}(\log y)^2 - \log w(2\log x - \log z) - \log y \log x \\ & +\frac{p}{4}(\log x)^2 - \frac{\pi^2}{3}\end{aligned}$$

From this we have algebraic equations as follows.

$$\begin{cases} \dfrac{x^{\frac{p}{2}} wz(xw-1)(x-y)(x-z)}{(x-yw)(x-zw)(x-yzw)} = 1 \\ \dfrac{(x-yw)(x-yzw)(yzw-1)}{x(x-y)(y-1)zw^2} = 1 \\ \dfrac{(x-zw)(x-yzw)(1-yzw)}{wy(x-z)(z-1)z} = 1 \\ \dfrac{(xw-1)(yw-x)(zw-x)(yzw-1)(yzw-x)}{(w-1)x^2y^2zw^2} = 1 \end{cases} \tag{A.3}$$

Using Mathematica 4.1, for every $p = 0, 1, \dots$ we can calculate the solutions of (A.3).
For $p = 0, 1, \dots 100$ we can see V_p in Table A.3 (p.64).

p	V_p	**Volume**	**CS**
0	$4.059766425\sqrt{-1}$	4.05976643	0
1	$0.22917210884 + 4.0863131024\sqrt{-1}$	4.086313102	0.22917210884
2	$0.4445419261 + 4.1639959336\sqrt{-1}$	4.163995934	0.4445419261
3	$0.63348406622 + 4.2886081226\sqrt{-1}$	4.288608123	0.63348406622
4	$0.7812534256 + 4.45391263891\sqrt{-1}$	4.4539126389	0.7812534256
5	$0.87062091766 + 4.64306000721\sqrt{-1}$	4.6430600072	0.87062091766
6	$0.8989379100 + 4.8250823231\sqrt{-1}$	4.825082323	0.8989379100
7	$0.88585969018 + 4.97820454177\sqrt{-1}$	4.9782045418	0.88585969018
8	$0.8524012829 + 5.0999246548\sqrt{-1}$	5.099924655	0.8524012829
9	$0.810967794 + 5.1955915341\sqrt{-1}$	5.195591534	0.810967794
10	$0.76770053942 + 5.2711863545\sqrt{-1}$	5.271186355	0.76770053942
11	$0.72547262686 + 5.331552910\sqrt{-1}$	5.33155291	0.72547262686
12	$0.68554893116 + 5.3803250646\sqrt{-1}$	5.380325065	0.68554893116
13	$0.6484042895 + 5.4201829083\sqrt{-1}$	5.420182908	0.6484042895
14	$0.6141256632 + 5.4531072787\sqrt{-1}$	5.453107279	0.6141256632
15	$0.5826136849 + 5.4805752561\sqrt{-1}$	5.480575256	0.5826136849
16	$0.5536854838 + 5.5037006282\sqrt{-1}$	5.503700628	0.5536854838
17	$0.5271275544 + 5.523333079\sqrt{-1}$	5.52333308	0.5271275544
18	$0.50272271413 + 5.5401282532\sqrt{-1}$	5.540128253	0.50272271413
19	$0.48026337471 + 5.5545975926\sqrt{-1}$	5.554597593	0.48026337471
20	$0.45955752094 + 5.5671441614\sqrt{-1}$	5.567144161	0.45955752094
21	$0.4404308094 + 5.57808866780\sqrt{-1}$	5.5780886678	0.4404308094
22	$0.4227266429 + 5.5876885849\sqrt{-1}$	5.587688585	0.4227266429
23	$0.4063052361 + 5.5961523532\sqrt{-1}$	5.596152353	0.4063052361
24	$0.3910422304 + 5.6036500394\sqrt{-1}$	5.603650039	0.3910422304
25	$0.3768271597 + 5.6103214174\sqrt{-1}$	5.610321417	0.3768271597
26	$0.3635619288 + 5.6162821507\sqrt{-1}$	5.616282151	0.3635619288
27	$0.3511593829 + 5.6216285663\sqrt{-1}$	5.621628566	0.3511593829
28	$0.3395420042 + 5.62644137105\sqrt{-1}$	5.6264413711	0.3395420042
29	$0.3286407464 + 5.6307885673\sqrt{-1}$	5.630788567	0.3286407464

Table A.3: The calculation for $M_p(6_3)$.

30	$0.318394004021 + 5.6347277591\sqrt{-1}$	5.634727759	0.3183940040206
31	$0.30874670736 + 5.6383079875\sqrt{-1}$	5.638307988	0.30874670736
32	$0.29964953221 + 5.6415712013\sqrt{-1}$	5.641571201	0.29964953221
33	$0.291058210325 + 5.6445534447\sqrt{-1}$	5.644553445	0.2910582103254
34	$0.2829329293 + 5.64728581935\sqrt{-1}$	5.6472858194	0.2829329293
35	$0.275237810452 + 5.6497952706\sqrt{-1}$	5.649795271	0.2752378104507
36	$0.2679404533 + 5.6521052322\sqrt{-1}$	5.652105232	0.2679404533
37	$0.26101154008 + 5.65423615814\sqrt{-1}$	5.6542361581	0.26101154008
38	$0.25442448875 + 5.6562059627\sqrt{-1}$	5.656205963	0.25442448875
39	$0.2481551515 + 5.6580303882\sqrt{-1}$	5.658030388	0.2481551515
40	$0.242181550143 + 5.6597233113\sqrt{-1}$	5.659723311	0.2421815501427
41	$0.23648364362 + 5.6612970008\sqrt{-1}$	5.661297001	0.23648364362
42	$0.2310431248 + 5.66276233505\sqrt{-1}$	5.6627623351	0.2310431248
43	$0.2258432413 + 5.6641289857\sqrt{-1}$	5.664128986	0.2258432413
44	$0.2208686368 + 5.6654055743\sqrt{-1}$	5.665405574	0.2208686368
45	$0.2161052118 + 5.6665998057\sqrt{-1}$	5.666599806	0.2161052118
46	$0.2115400003 + 5.66771858160\sqrt{-1}$	5.6677185816	0.2115400003
47	$0.20716105976 + 5.6687680987\sqrt{-1}$	5.668768099	0.20716105976
48	$0.20295737369 + 5.669753933439\sqrt{-1}$	5.669753933	0.20295737369
49	$0.1989187654 + 5.6706811140\sqrt{-1}$	5.670681114	0.1989187654
50	$0.195035820613 + 5.6715541841\sqrt{-1}$	5.671554184	0.1950358206133
⋮	⋮	⋮	⋮
100	$0.098397659903 + 5.68760068694\sqrt{-1}$	5.6876006869	0.0983976599029

Table A.3 (continued)

If p is negative, then we can check the following formula is numerically true,

$$V_p = \mathrm{CS}(M_p(6_3)) + \mathrm{Vol}(M_p(6_3))\sqrt{-1} = -\mathrm{CS}(M_{-p}(6_3)) + \mathrm{Vol}(M_{-p}(6_3))\sqrt{-1}\,.$$

Here second equality is true because knot 6_3 is achiral.

Bibliography

[1] Y. Akutsu, T. Deguch, and T. Ohtsuki, *Invariants of colored links*, J. Knot Theory Ramifications **1** (1992), no. 2, 161-184.

[2] J. E. Andersen and S. K. Hansen, *Asymptotics of the quantum invariants for surgeries on the figure 8 knot*, arXiv:math.GT/0506456.

[3] R. Benedetti and C. Petronio, *Lectures on hyperbolic geometry*, Universitext, Springer-Verlag, Berlin, 1992.

[4] R.H. Crowell and R.H. Fox, *Introduction to knot theory*, Graduate Texts in Mathematics **57**, Springer-Verlag, New York-Heidelberg, 1977.

[5] D.B.A. Epstein and R.C. Penner, *Euclidean decompositions of noncompact hyperbolic manifolds*, J. Differential Geom. **27** (1988), no. 1, 67-80.

[6] S. Garoufalidis and TTQ. Le, *On the volume conjecture for small angles* , preprint, arXiv:math.GT/0502163.

[7] S. Garoufalidis and TTQ. Le, *An analytic version of the Melvin-Morton-Rozansky conjecture*, arXiv:math.GT/0503641.

[8] S. Garoufalidis and TTQ. Le, *Asymptotics of the colored Jones function of a knot*, arXiv:math.GT/0508100.

[9] S. Gukov, *Three-Dimensional Quantum Gravity, Chern-Simons Theory, and the A-polynomial*, HUTP-03/A003, ITEP-TH-50/02, arXiv:hep-th/0306165.

[10] R. M. Kashaev, *The hyperbolic volume of knots from the quantum dilogarithm*, Lett. Math. Phys. **39** (1997), no. 3, 269–275.

[11] R. M. Kashaev and O. Tirkkonen, *Proof of the volume conjecture for torus knots*, J. Math. Sci. 115(2003), 2033-2036.

[12] C. Kassel, *Quantum groups*, Graduate Texts in Math. **155**, Springer-Verlag, 1994.

[13] R. Kirby and P. Melvin, *The 3-manifold invariants of Witten and Reshetikhin-Turaev for* $sl(2,\mathbb{C})$, Invent. Math. **105** (1991), 473-545.

[14] K. Habiro, *On the colored Jones polynomials of some simple links*, Recent progress towards the volume conjecture (Japanese) (Kyoto, 2000). Sūrikaisekikenkyūsho Kōkyūroku No. **1172** (2000), 34–43.

[15] J. Hoste and P.D. Shanahan, *Trace fields of twist knots*, J. Knot Theory Ramifications **10** (2001), no. 4, 625-639.

[16] V. F. R. Jones, *A polynomial invariant for knots via von Neumann algebras*, Bull. Amer. Math. Soc. **12** (1985), 103-111.

[17] L. Lewin, *Polylogarithms and associated functions*, North-Holland Publishing Co. , New York-Amsterdam, 1981.

[18] G. Masbaum, *Skein-theoretical derivation of some formulas of Habiro*, Algebr. Geom. Topol. 3 (2003), 537–556.

[19] A. D. Mednykh, *On hyperbolic and spherical volumes for knot and link cone-manifolds*, Kleinian groups and hyperbolic 3-manifolds (Warwick, 2001), 145–163, London Math. Soc. Lecture Note Ser., 299, Cambridge Univ. Press, Cambridge, 2003.

[20] R. Meyerhoff and W.D. Neumann, *An asymptotic formula for the eta invariants of hyperbolic* 3*-manifolds*, Comment. Math. Helv. 67 (1992), no. 1, 28–46.

[21] H. Murakami, *Kashaev's invariant and the volume of a hyperbolic knot after Y. Yokota*, Physics and combinatorics 1999 (Nagoya), 244–272, World Sci. Publishing, River Edge, NJ, 2001.

[22] H. Murakami, *Optimistic calculations about the Witten-Reshetikhin-Turaev invariants of closed three-manifolds obtained from the figure-eight knot by integral Dehn surgeries*, Recent progress towards the volume conjecture (Kyoto, 2000). Sūrikaisekikenkyūssho Kōkyūroku (2000), no.**1172** , 85-104.

[23] H. Murakami, *Some limits of the colored Jones polynomials of the figure-eight knot*, Kyungpook Math. J. 44 (2004), no. 3, 369–383.

[24] H. Murakami, *The colored Jones polynomials and the Alexander polynomial of the figure eight knot*, arXiv:math.GT/0502428.

[25] H. Murakami and J. Murakami, *The colored Jones polynomials and the simplicial volume of a knot*, Acta Math. **186** (2001), no. 1, 85–104.

[26] H. Murakami and J. Murakami and M. Okamoto and T. Takata and Y. Yokota, *Kashaev's conjecture and the Chern-Simons invariants of knots and links*, Experiment. Math. **11** (2002), no. 3, 427–435.

[27] H. Murakami and Y. Yokota, *The colored Jones polynomials of the figure-eight knot and its Dehn surgery spaces,* arXiv:math.GT/0401084.

[28] W.D. Neumann and A.W. Reid, *Arithmetic of hyperbolic manifolds*, Topology '90 (Columbus, OH, 1990), 273–310, Ohio State Univ. Math. Res. Inst. Publ., 1, de Gruyter, Berlin, 1992.

[29] W.D. Neumann and D. Zagier, *Volumes of hyperbolic 3-manifolds*, Topology **24** (1985), no. 3, 307-332.

[30] K. Ohnuki, *The colored Jones polynomial of 2-bridge link and hyperbolicity equation of it's complements*, J. Knots Theory Ramifications **14** (2005), no. 6, 751-773.

[31] T. Ohtsuki, *Quantum invariants, A study of knots and 3-manifolds, and their sets*, World Scientific Publishing, 2002.

[32] J. G. Ratcliffe, *Foundations of hyperbolic manifolds*, Graduate Texts in Mathematics, **149**, Springer-Verlag, New York, 1994.

[33] D. Rolfsen, *Knots and links*, Mathematics Lecture Series, No **7**, Publish or Perish, Inc., Berkeley, Calif., 1976.

[34] M. Sakuma and J.Weeks, *Examples of canonical decompositions of hyperbolic link complements*, Japan. J. Math. (N.S.) **21** (1995), no. 2, 393–439.

[35] D. Thurston, *Hyperbolic volume and the Jones polynomial*, abstract of the lecture at "Invariants de noeuds et de variétés de dimension 3"(1999), I.E.S.A.-G.

[36] W. Thurston, *The geometry and topology of three-manifolds*, Prinston University press (1979).

[37] J. Weeks, *Convex hulls and isometries of cusped hyperbolic* 3*-manifolds*, Topology Appl. **52** (1993), no. 2, 127-149.

[38] J. Weeks, SnapPea.

[39] Y. Yokota, *On the volume conjecture for hyperbolic knots*, preprint, available at www.comp.metro-u.ac.jp/ jojo/

[40] Y. Yokota, *On the potential functions for the hyperbolic structures of a knot complement*, Geometry and Topology Monographs, vol. 4 (2002), 303–311.

List of Papers by Koji Ohnuki

[1] K. Ohnuki, *The colored Jones polynomial of 2-bridge link and hyperbolicity equation of it's complements*, J. Knot Theory Ramifications **14** no. 6, 751–773, 2005.